Deep–Sea Research I 190 (2022) 103892

Contents lists available at ScienceDirect

Deep-Sea Research Part I

journal homepage: www.elsevier.com/locate/dsri

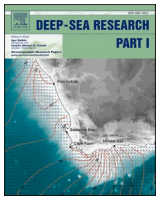

Spatial and temporal distribution of cold-water corals in the Northeast Atlantic Ocean over the last 150 thousand years

Maria Luiza de Carvalho Ferreira [a,*], Laura F. Robinson [a], Joseph A. Stewart [a], Tao Li [b], Tianyu Chen [b], Andrea Burke [c], Marcelo V. Kitahara [d,e], Nicholas J. White [f]

[a] School of Earth Science, University of Bristol, Queens Road, Bristol, BS8 1RJ, UK
[b] MOE Key Laboratory of Surficial Geochemistry, Department of Earth and Planetary Sciences, Nanjing University, Nanjing, China
[c] School of Earth and Environmental Sciences, University of St Andrews, St Andrews, UK
[d] Institute of Marine Science, Federal University of São Paulo, Santos, SP, 11070-100, Brazil
[e] Centre for Marine Biology, University of São Paulo, São Sebastião, SP, 11612-109, Brazil
[f] Bullard Laboratories, Department of Earth Sciences, University of Cambridge, Cambridge, UK

ARTICLE INFO

Keywords:
U-Th dating
Coral biogeography
Northeast Atlantic
Last glaciation
Last deglaciation
Holocene

ABSTRACT

Scleractinian cold-water corals are found across the Northeast Atlantic, providing structure for important habitats that support high biodiversity. Climate-driven perturbations on parameters such as carbonate chemistry, oxygen, bottom currents, productivity and temperature have the potential to impact the abundance and diversity of these cold-water coral communities. One way to explore the linkage between corals and climate is to examine historic coral distributions during times of past climate change. Previous coral dating efforts in the Northeast Atlantic (n ~ 700) have focused on reef-forming colonial coral communities from shelf and slope areas. However, there are far fewer data from open-ocean settings or from solitary coral species, thus precluding assessment of basin-wide controls on coral occurrence. Here, we contribute >600 new U-series ages for both solitary and colonial coral species from open-ocean sites including the Reykjanes Ridge and seamounts in the mid and low latitudes to map the changing distribution of Northeast Atlantic cold-water corals over the last 150,000 years. The temporal occurrences of solitary and colonial corals from our offshore sites are broadly similar to the distributions along the nearer-shore sites at the same latitudes. In the cold-temperate and high-latitude Northeast Atlantic, corals are most abundant during warm climate intervals, with the Reykjanes Ridge (60°N) representing the northernmost limit of corals in the Northeast Atlantic during Marine Isotope Stage (MIS) 5, MIS 3 and Bølling-Allerød. This biogeographical distribution expanded northwards to the Norwegian margin at the onset of the Holocene when the ice sheets retreated and modern-like oceanographic conditions were established. We interpret the abundance of corals at these northerly sites to be linked with increased food supply and favourable hydrological conditions. By contrast, coral sites south of 45°N are characterised by glacial and deglacial occurrences, with a marked decline during the Holocene. This distribution is also linked to food supply, potentially driven by shifts in dust fertilization and upwelling, in addition to changes in dissolved oxygen concentration and temperature. Together, these findings emphasize the links between climate, oceanic processes, and cold-water coral distribution, pointing to low food supply and low oxygen concentration as limiting factors for cold-water coral populations. Both parameters are changing in the modern ocean, with implications for future coral communities.

1. Introduction

Ecosystem interactions with the climate system are a complex topic of much interest in the scientific literature (Blois et al., 2013; Canadell et al., 2021). Marine life is influenced by climate change, for example by habitat gain or loss (Henry et al., 2014), but marine species can also contribute to the modulation of climate via their role in carbon cycling (e.g., Sigman and Hain, 2012). With rising atmospheric CO_2 the ocean is warming, whilst seawater pH and saturation state are reducing (Canadell et al., 2021), triggering changes to the food web, for instance

* Corresponding author.
E-mail address: malu.ferreira@bristol.ac.uk (M.L. de Carvalho Ferreira).

https://doi.org/10.1016/j.dsr.2022.103892
Received 22 November 2021; Received in revised form 28 September 2022; Accepted 1 October 2022
Available online 6 October 2022

decreasing primary production in the North Atlantic (Capuzzo et al., 2018). These changes have stimulated research into the effects of rapid climate change on marine fauna (e.g., Miller et al., 2011). One way to investigate the interactions between ecosystems and the marine environment is to look back in the past (Hebbeln et al., 2019), comparing well-dated coral samples with paleoclimate records from intervals of climate change (Stewart et al., 2021; Thiagarajan et al., 2013).

Cold-water corals are keystone taxa that can form structural habitats for diverse and abundant marine fauna (Roberts et al., 2006). In addition, their carbonate skeletons can be dated using radiometric techniques, and the ages can then be used to reconstruct the timing of coral mound formation and changing coral population distributions over tens of thousands of years (Douarin et al., 2013; Eisele et al., 2008; Margolin et al., 2014; Mienis et al., 2009; Thiagarajan et al., 2013; Titschack et al., 2015; Victorero et al., 2016; Wienberg et al., 2009). In the Northeast Atlantic there are about 700 published coral ages, primarily from colonial species sampled on continental shelves and slopes (Table 1). These data have shown that the spatial and temporal distribution of cold-water coral communities changed with timings aligned with major global climate change events (Frank et al., 2011; Schröder-Ritzrau et al., 2005). For example, during glacial and deglacial intervals corals thrived in tropical and warm-temperate latitudes of the Northeast Atlantic (Eisele et al., 2011; Frank et al., 2011; Schröder-Ritzrau et al., 2005; Wienberg et al., 2018), but these communities decreased in abundance at the onset of the Holocene. By contrast, the opposite behaviour has been detected in northerly regions (>45°N) such as the colder and more productive Celtic and Nordics Seas where prolific cold-water coral reefs were established or re-colonised at the onset of the Holocene (Dorschel et al., 2005, 2007; Eisele et al., 2008; Van der Land et al., 2010; Wienberg et al., 2020; Bonneau et al., 2018; De Mol et al., 2011; Douarin et al., 2013; López Correa et al., 2012; Mienis et al., 2009; Raddatz et al., 2016; Victorero et al., 2016). With growing evidence for climate-induced latitudinal displacement of cold-water coral populations in the Northeast Atlantic over the last 150,000 years (Frank et al., 2009, 2011; Schröder-Ritzrau et al., 2005; Wienberg et al., 2010) it is important to consider the impact of ongoing changing environmental conditions on coral and coral associated communities.

Scleractinian cold-water corals are suspension-feeders that rely on food supply from particulate organic matter either falling from surface water primary production or brought in by the hydrodynamic action of bottom currents (Davies and Guinotte, 2011; Mohn et al., 2014; Morato et al., 2020; Roberts et al., 2006). As a result, modern framework-forming cold-water coral distributions occur preferentially within high productivity and high energy areas (Freiwald, 2002; Mohn et al., 2014). Other factors important to coral health may include dissolved oxygen concentration (Dodds et al., 2007; Stewart et al., 2021; Thiagarajan et al., 2013), carbonate saturation state (Guinotte et al., 2006; Thiagarajan et al., 2013), and seawater density gradients (associated with temperature and salinity characteristics of water masses; De Mol et al., 2011; Dullo et al., 2008; Flögel et al., 2014). Bottom currents can also play a role in the dispersal of coral larvae (Henry et al., 2014). Complicating the picture, recent findings raise questions about the limiting environmental conditions that cold-water corals can withstand. Unexpectedly, thriving cold-water reefs have been found under hypoxic and warm conditions off the Angola margin (Southeast Atlantic; Hanz et al., 2019; Hebbeln et al., 2020; Orejas et al., 2021). There, coral success has been linked to the high abundance and quality of organic matter as a food source (Hanz et al., 2019).

A combination of factors is needed to explain coral population distributions – both today and in the past. For example, the success of coral communities in the southern Gulf of Cádiz is thought to be related to productivity, which in turn is driven by a combination of enhanced dust input and frontal upwelling (Foubert et al., 2008; Wienberg et al., 2009, 2010). In the Holocene a frontal zone shift and an increase in seawater temperature have been linked to the subsequent demise of the coral population (Wienberg et al., 2010). The development of coral mounds

Table 1
List of references used for the cold-water coral compilation from Northeast Atlantic Ocean coral sites. Reference numbers correspond to locations in Fig. 1.

Regions	Latitude range (°N)	Ref. number	References	Location
Norwegian shelf	70°49′N to 59°N	1	Raddatz et al. (2016)	Lopphavet, Oslofjord and Sula Reef
		2	López Correa et al. (2012)	Trænadjupet and Stjernsund
		3	Schröder-Ritzrau et al. (2005)	Kosterfjord and Sula Reef
		20	Frank et al. (2011)	Trænadjupet
		24	Titschack et al. (2015)	Stjernsund, Træna and Røst Reef
		30	Lindberg and Mienert (2006)	Fugløy Reef
Northern Northeast Atlantic	62°56′N to 42°47′N	4	Douarin et al. (2013)	Scottish margin
		5	Frank et al. (2004)	Rockall Trough
		6	Frank et al. (2009)	Porcupine Seabight
		20	Frank et al. (2011)	Porcupine Seabight
		7	Dorschel et al. (2007)	Porcupine Seabight
		8	de Mol et al. (2011)	Bay of Biscay
		9	Schröder-Ritzrau et al. (2003)	Rockall Trough Bay of Biscay
		3	Schröder-Ritzrau et al. (2005)	Faroe Island Porcupine Seabight
		22	van der Land et al. (2010)	Rockall Trough
		23	van der Land et al. (2014)	Porcupine Seabight
		25	Bonneau et al. (2018)	Rockall Trough
		26	Victorero et al. (2016)	Rockall Trough
		27	Wienberg et al. (2020)	Porcupine Seabight
		28	Eisele et al. (2008)	Porcupine Seabight
		29	Mienis et al. (2009)	Rockall Trough
mid-North Atlantic	42°N to 33°12′N	10	Adkins et al. (1998)	mid-North Atlantic
		11	Eltgroth et al. (2006)	mid-North Atlantic
		9	Schröder-Ritzrau et al. (2003)	Azores
Gulf of Cádiz	36°11′N to 35°N	12	Wienberg et al. (2009)	Gulf of Cádiz
		13	Wienberg et al. (2010)	Gulf of Cádiz
		9	Schröder-Ritzrau et al. (2003)	Gulf of Cádiz
		3	Schröder-Ritzrau et al. (2005)	Gulf of Cádiz
		20	Frank et al. (2011)	Gulf of Cádiz
		21	Dubois-Dauphin et al. (2016)	Gulf of Cádiz
Temperate seamounts	36°58′N to 29°49′N	9	Schröder-Ritzrau et al. (2003)	Lars Seamount Conception Seamount
		3	Schröder-Ritzrau et al. (2005)	Galicia Bank Conception Seamount Lars Seamount Ampère Seamount

(continued on next page)

Table 1 (*continued*)

Regions	Latitude range (°N)	Ref. number	References	Location
				Last Minute Seamount
				Josephine Seamount
				Lion Seamount
				Annika Seamount
				Unicorn Seamount
				Filho do Funchal
Mauritania margin	20°15′N to 17°29′N	14	Wienberg et al. (2018)	off Mauritania
		15	Eisele et al. (2011)	off Mauritania
Northeast Equatorial Atlantic	9°13′N to 2°19′N	16	Mangini et al. (1998)	Equatorial Atlantic
		17	Chen et al. (2015)	Equatorial Atlantic
		18	Chen et al. (2016)	Equatorial Atlantic
		19	Chen et al. (2020)	Equatorial Atlantic

along the Mauritanian margin during the last glacial and deglacial has also been linked to increased surface ocean productivity (Eisele et al., 2011). However, dissolved oxygen and temperature may also have been important factors. For instance modern corals are only found inhabiting canyons off Mauritania, where cascading events are thought to episodically deliver food and well-oxygenated waters from the surface to the deep (Wienberg et al., 2018).

Thus far, most data from the Northeast Atlantic come from reef-forming cold-water corals along the continental margin. The few ages from seamounts in the open-ocean and/or from solitary corals are generally in line with the timing of observations from shelf areas, suggesting that there could be a common controlling mechanism across the basin (Frank et al., 2011; Schröder-Ritzrau et al., 2003, 2005; Wienberg et al., 2009, 2010). However, the limited data from these open-ocean sites or from solitary species prevent us from determining whether nearshore mound forming communities are being controlled by local (e.g., coastal upwelling and local productivity change) or basin-wide processes that would dictate scleractinian cold-water coral occurrence regardless of species or habitat type.

Here we present 616 new ages obtained from solitary and colonial scleractinian cold-water corals from open-ocean habitats including volcanic ridges and seamounts in the Northeast Atlantic. These sites provide a direct contrast to the majority of existing data from the region. Our new coral ages, combined with ~700 existing published data from the Norway shelf to the Mauritanian margin, represent the most up to date temporal distribution of cold-water corals from the Northeast Atlantic. We use this combined dataset to test whether productivity (food supply) is the major control on cold-water corals, including an assessment of basin-wide patterns and potential differences between the continental margin and open ocean settings, and solitary and reef forming species over the last 150 thousand years.

2. Site descriptions

The new U-series ages obtained from scleractinian cold-water corals come from three locations: the Reykjanes Ridge (57°N to 61°N, 28°W to

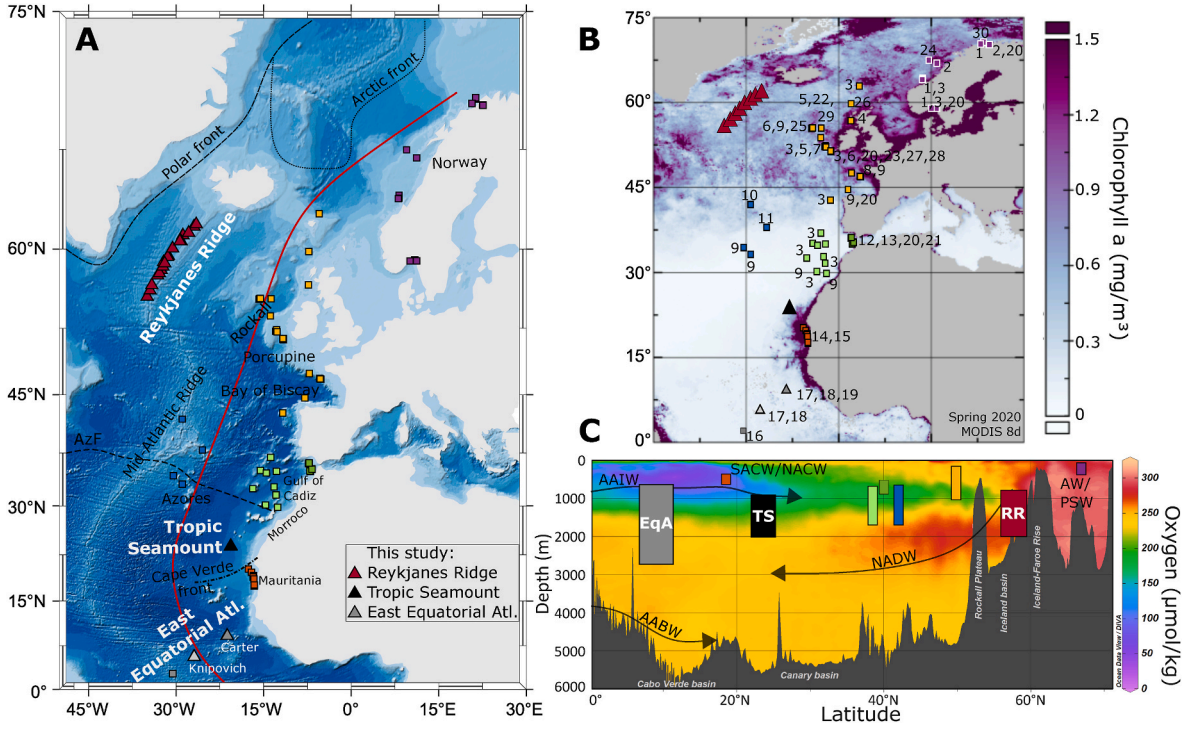

Fig. 1. Locations of available cold-water corals discussed in the text, and oceanic parameters. (A) Cold-water coral records presented in main discussion. Published (squares) and new records (triangles) from Tropic Seamount (black), East Equatorial Atlantic (grey) and Reykjanes Ridge (red). Regions are grouped by colour (purple to Norwegian shelf, yellow to northern Northeast Atlantic, blue for mid-North Atlantic, dark green for Gulf of Cádiz, light green for temperate seamounts, and orange for Mauritania margin, see Table 1 for details). Dashed lines indicate modern position of Polar and Arctic fronts (Eynaud et al., 2009). Red line indicates profile section illustrated in Panel C. (B) Chlorophyll-a concentration map (from MODIS Aqua 8-daily resolution, period of March to June 2020 at https://giovanni.gsfc.nasa.gov; Panoply). Numbers correlate to the references used for cold-water coral compilation listed in Table 1. (C) Dissolved oxygen profile (Olsen et al., 2020; GLODAP) depth distribution of corals from each region (indicated by same colour as map) and position of main water masses. AAIW, Antarctic Intermediate Water; AABW, Antarctic Bottom Water; SACW/NACW, South and North Central Water; NADW, North Atlantic Deep Water; AW, Atlantic Water; PSW, Polar Surface Water.

33°W); the Tropic Seamount (23°55′N, 20°45′W); and the East Equatorial Atlantic from Carter (9°N, 21°W) and Knipovich seamounts (5°N, 27°W; Fig. 1, Table 2). Fossil and living corals from Reykjanes Ridge were collected from 35 dredge sites along the axis and western flank of this part of the Mid-Atlantic Ridge. The presence of modern cold-water corals at Reykjanes Ridge has been previously documented, with high species richness but smaller colonies compared to higher latitude shelf areas (Mortensen et al., 2008). Corals from Tropic Seamount (extending from 4100 m to its summit around 1000 m) were collected by ROV *Isis* from the seamount top and the upper part of the flanks (down to 1800 m; Murton, 2016). The known modern coral population consists of solitary corals (e.g., *Javania cailleti* presented in this study) and small colonies of *Solenosmilia variabilis,* which have a patchy distribution along ledges. Rich coral gardens mostly consisting of octocorals are found at the eastern and western sites of the seamount (Murton, 2016; Ramiro-Sánchez et al., 2019). The corals from the Equatorial Atlantic seamounts were also collected by ROV *Isis* (Chen et al., 2015, 2016, 2020; Robinson, 2014) during 16 dives at five sites, however only data from seamounts in the Northeast Atlantic are presented in this study (Carter and Knipovich; some authors refer to Carter Seamount as Annan Seamount (e.g., Victorero et al., 2018). On these seamounts, the modern occurrences of scleractinian corals are patchy, with dense octocoral gardens and *Enallopsammia* sp. observed, particularly on the southern edge of Carter Seamount (Victorero et al., 2018).

2.1. Oceanographic settings

2.1.1. Reykjanes Ridge

The bathymetry of the Reykjanes Ridge controls the modern position of the Sub-Arctic Front, corresponding to the maximum extent of winter drift sea-ice (Moros et al., 2012). This front marks the interaction between the warm, saline waters of the poleward flowing North Atlantic Current (NAC), and the cold and relatively fresh polar waters flowing southward along the Greenland margin. The intermediate waters mostly consist of Labrador Sea Water (Rhein et al., 2002), and a smaller contribution of Subpolar Mode Water that includes recirculated central waters transported by the NAC and modified by sea-ice interaction to a cold, fresh and nutrient-rich water (García-Ibáñez et al., 2015). The deeper layers include denser, oxygen-rich overflow waters from the Nordic Seas (Iceland- Scotland Overflow Water and Denmark Strait Overflow Water; de Carvalho Ferreira and Kerr, 2017). The corals in this study are from the intermediate and deep layers within the influence of these northern-sourced water masses (Fig. 1).

2.1.2. Tropic Seamount and east Equatorial Atlantic sites

Tropic Seamount is situated in the southern Canary Island Seamount Province around 500 km from the Northwest African coast which is a highly-productive upwelling region (Romero et al., 2008). The eutrophic upwelled waters are exported offshore as upwelling filaments and eddies as far as Tropic Seamount (Hernández-Guerra et al., 2005, Fig. 1). Additionally, subsurface particle-rich layers (enriched in organic matter) extend as far as 600 km offshore from the African shelf between 400 m and 800 m depth (Karakaş et al., 2006), potentially acting as a food source for corals.

The sites within the east Equatorial Atlantic are within the zonal Equatorial Current system, the modern position of the Intertropical Convergence Zone and the African dust plume (Fig. S1). Dust and nutrient-rich upwelling waters fertilize the surface ocean, stimulating primary productivity (Zarriess and Mackensen, 2010). Dust dispersion is controlled by the trade winds and continental aridity, on seasonal as well as millennial-scales.

The upper water column of these low latitude sites comprises warm surface (0–50 m) and thermocline (<700 m) waters, which include North Atlantic Central Water and South Atlantic Central Water (Pastor et al., 2015). The modern oxygen minimum zone lies between 600 m and 1000 m within the boundary between the thermocline waters and Antarctic Intermediate Water (AAIW). AAIW is recognized by its low salinity and high dissolved silicate sourced from the Southern Ocean (de Carvalho Ferreira and Kerr, 2017; Pastor et al., 2015). Deeper layers (>1500 m) predominantly consist of North Atlantic Deep Water (NADW). In the context of the modern hydrography, the cold-water corals from both sites are within AAIW (approx. 600 m–1500 m) and NADW.

Table 2
Site, sampling, and taxa information of cold-water coral sites presented in this study. Depth of Reykjanes Ridge samples corresponds to the mean depth of dredge on and off bottom. Taxa corresponds to all identified species.

Location	Lat. (°N)	Lon. (°W)	Depth (m)	Cruise	Year	Sampling method	Taxa
Reykjanes Ridge (125 ages)	57 to 61	28 to 33	768 to 2022	CE08-06	2008	dredge	*Madrepora* sp. *Desmophyllum pertusum* *Solenosmilia* sp. *Desmophyllum dianthus* *Caryophyllia* sp. *Flabellum* sp.
Tropic Seamount (36 ages)	23°55′	20°45′	970 to 1797	JC142	2016	ROV	*Desmophyllum dianthus* *Solenosmilia variabilis* *Caryophyllia* sp. *Javania caelleti* *Madrepora oculata*
Carter Seamount - East Equatorial Atlantic (308 ages)	9	21	639[a] to 2160	JC094	2013	ROV	*Caryophyllia* sp. *Desmophyllum dianthus* *Enallopsammia* sp. *Javania* sp. *Madrepora* sp. *Polymyces* sp.
Knipovich Seamount - East Equatorial Atlantic (132 ages)	5	26	749 to 2599[b]	JC094	2013	ROV	*Dasmosmillia* sp. *Caryophyllia* sp. *Desmophyllum dianthus* *Enallopsammia* sp. *Javania* sp.

[a] One sample collected at 265 m.
[b] One sample collected at 2814 m.

3. Dating methods

Two U-series methods were applied to date the new samples. U-series laser ablation dating was used to provide a rapid determination of coral age (Spooner et al., 2016). Other samples were dated by more accurate and precise U-series isotope-dilution (per-mil versus per-cent level for the laser ablation dating; Cheng et al., 2000; Spooner et al., 2016).

The samples dated by U-series laser ablation were cut and polished before ablation using a Photon Machines Analyte G2 193 nm laser. The ^{230}Th and ^{238}U isotopes were measured simultaneously using a Neptune Multi-Collector Inductivity Coupled Plasma Mass Spectrometer (MC-ICP-MS) on a central ion counter and a Faraday cup respectively (Spooner et al., 2016). Final ages were calculated solely on measured ^{230}Th/^{238}U ratios, thus assuming that there has been no open-system behaviour and that its initial ^{230}Th is negligible (Spooner et al., 2016). The age was calculated by the Newton-Raphson iteration method, using the (^{230}Th/^{238}U) of the sample corrected for background (laser cell gas blank) and scaled to an in-house inorganic aragonite standard (Table S1; Spooner et al. (2016).

For U-series isotope-dilution dating, approximately 0.15 g of sample was physically cleaned and then oxidatively and reductively cleaned following established chemical protocols (Cheng et al., 2000). Once clean, the samples were dissolved in HNO_3 (7.5 M) and gravimetrically-spiked with a^{236}U–^{229}Th mixed spike calibrated to uncertainty of 4.1‰ (2s; Burke and Robinson, 2012). U and Th in samples were co-precipitated with Fe-hydroxide, then separated and purified by anion-exchange columns (Chen et al., 2015). The U and Th were measured separately by bracketing standard methods (international U standard U112a and in-house Th standard SGS) on a Neptune MC-ICP-MS. Repeat analysis of the Harwell uraninite standard HU1 (uranium) and ThB (in-house thorium solution of ^{229}Th, ^{230}Th, ^{232}Th; Auro et al., 2012) standards gave an accuracy of 1‰ (1*s*) and long-term reproducibility of 1.3‰ (1*s*) for both ^{238}U/^{234}U and ^{230}Th/^{229}Th. Additionally, a pure ^{236}U spike was added to the Th fraction to allow measurement of ^{230}Th and ^{229}Th by ^{236}U normalization (Chen et al., 2015). The final ages were calculated iteratively, solved 100,000 times by Monte Carlo simulation and corrected for initial ^{230}Th using the (^{232}Th/^{230}Th) atomic ratio of 12,500 based on modern seawater ratios (Cheng et al., 2000; Robinson et al., 2005). All dates are given as years before present (BP), where the present is the calendar year 1950 (Table S2).

Previously published U–Th ages (n = 580) were included following the original publication. We did not apply the quality controls that we applied to our samples (e.g., initial δ^{234}U, [^{238}U] and [^{232}Th], see Section 4.1) to these compiled coral data, since similar issues were addressed in the relevant publications. Within the compilation there are a few datapoints (n = 20) which fall outside our 15‰ initial δ^{234}U tolerance (see Section 4.1), however inclusion or exclusion of these data does not change our overall findings. Radiocarbon ages (n = 85; Douarin et al., 2013; Frank et al., 2004; Titschack et al., 2015; Victorero et al., 2016; Wienberg et al., 2020, 2009) were re-calibrated using the Calib8.1 software and the new Marine20 calibration curve (Heaton et al., 2020). To account for the offset between deep water and surface water radiocarbon in the past we apply an offset from the contemporaneous Marine20 value (Table S3; details in supplementary material). When the original, non-calibrated ^{14}C ages were not reported in the original publication (n = 12; Frank et al., 2011, 2009), we used the reported calibrated ages.

4. Results

4.1. Dating results and data quality

4.1.1. U-series laser ablation ages

A total of 140 samples from Reykjanes Ridge and 434 samples from the east Equatorial Atlantic were dated by U-series laser ablation and yielded ages from 150 kyr BP to 0.3 kyr BP (Table S1). Spooner et al. (2016) reported expected uncertainties based on coral isotopic heterogeneity and counting statistics to be approximately ±0.8 kyr, ±1.5 kyr and ±15 kyr at 10 kyr BP, 20 kyr BP and 125 kyr BP, respectively (Fig. S2). We use these assumptions as a basis for the acceptable upper age limit for our samples, with ages with uncertainties above this level being rejected. Samples younger than 1 kyr BP were included in the compilation only when the absolute error was lower than the calculated age. In total, 44 sample ages were rejected (n = 31 Reykjanes Ridge and n = 13 east Equatorial Atlantic) resulting in 530 U-series laser ablation ages (n = 109 Reykjanes Ridge and n = 421 east Equatorial Atlantic; Table S1) included to the final database. Even if these ages had been included, there would be no change to the overall interpretation.

4.1.2. U-series isotope dilution ages

U-series isotope-dilution ages (n = 118, including duplicates) ranged from 148 kyr BP to 0.1 kyr BP (Table S2). The [^{232}Th] from Tropic Seamount samples averaged 2.9 ppb (maximum 16.8 ppb), from Reykjanes Ridge averaged 0.9 ppb (max 3.9 ppb) and from east Equatorial Atlantic averaged 4.2 ppb (max 18.1 ppb). We applied three quality control measures: concentration of ^{232}Th; concentration of ^{238}U; and the initial δ^{234}U ($\delta^{234}U_i = \delta^{234}U \times e^{(\lambda_{234} t)}$). The 86 U-series isotope dilution ages (n = 36 Tropic Seamount, n = 32 Reykjanes Ridge, n = 18 east Equatorial Atlantic) which pass these quality measures were included in the final database. Where replicate measurements are available, the highest quality sub-sample for each coral was selected based on quality control parameters described below (Table S2).

Samples with [^{232}Th] >6 ppb were not included in the compilation because of the large associated age uncertainty (Table S2), though inclusion of these data would not change the main findings. Four samples from Tropic Seamount showed anomalously low ^{238}U concentrations (<1.6 ppm) and were also not included in the compilation (Table S2). We inferred from trace metal analysis that two of these samples included high magnesium calcite, perhaps from encrusting organisms such as bryozoans.

The $\delta^{234}U_i$ screening criterion was used to assess open-system behaviour resulting from diagenetic alteration (Cheng et al., 2000; Robinson et al., 2006). The $\delta^{234}U_i$ results (Fig. S3, Table S2) for the majority of our samples are within 10‰ of modern seawater values (146.8 ± 0.1‰; Andersen et al., 2010), within the expected variability range for the seawater over the past 360 kyr (~15‰; Chen et al., 2015; Henderson, 2002). Three samples (two from Tropic Seamount and one from Reykjanes Ridge; Table S2) were thought to be affected by diagenetic alteration because they fall outside the expected variation range of seawater (±15‰ from modern seawater; Henderson, 2002) thus they were excluded from the compilation.

4.2. Temporal distribution of corals at new sites

4.2.1. Reykjanes Ridge

Coral samples from Reykjanes Ridge (n = 141) ranged in age from 110 kyr BP to recent. Colonial corals were found only after 13.9 kyr BP, while solitary corals clustered in four time intervals within MIS 5, 3 and 1 (Fig. 2). Three samples dated within the interval of 110 to 95 kyr BP, and eight samples between 80 and 70 kyr BP. In the following age cluster, the corals fall within 55 to 35 kyr BP (Fig. 3). There are no corals from 35 to 15 kyr BP. The youngest age cluster extends from the onset of the Bølling-Allerød (B-A, 14.7 to 13 kyr BP; Fig. 3) to recent, when corals show distinct peak for both solitary and colonial forms during the last 2 kyr BP (Fig. 2).

4.2.2. Tropic Seamount

Tropic Seamount cold-water corals dated from 148 to 0.1 kyr BP (n = 36), with two live-collected samples (Fig. 2). Solitary corals were found at (i) 56 kyr BP, (ii) 34 to 12 kyr BP, and (iii) recent. Colonial corals comprise four age ranges: (i) 150 to 140 kyr BP, (ii) around 82 kyr

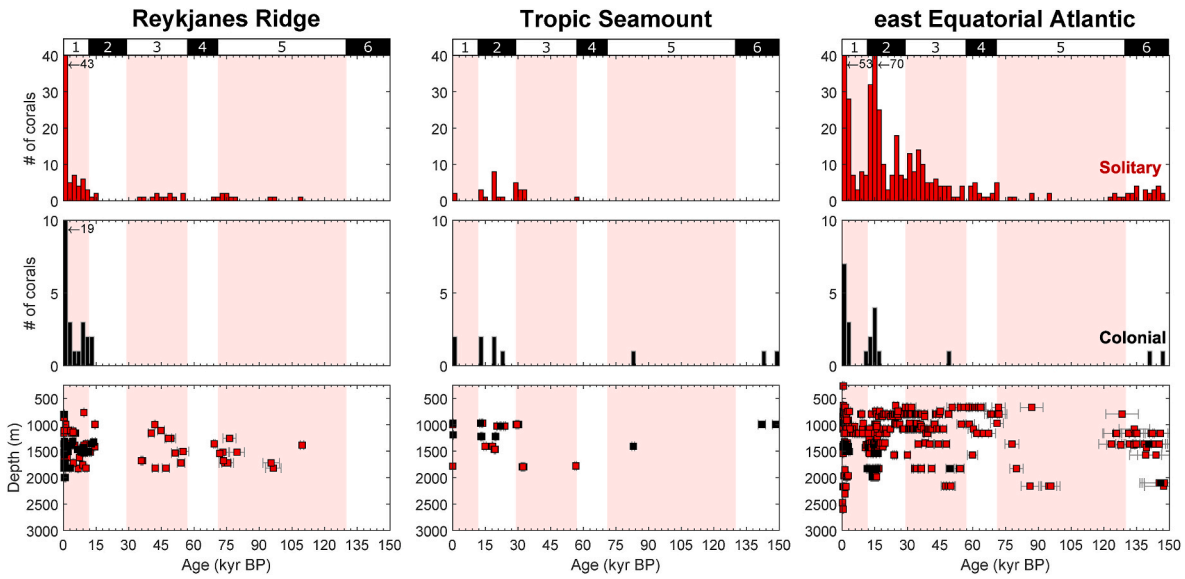

Fig. 2. Age distribution of new U-series dated cold-water corals from Reykjanes Ridge (n = 141), Tropic Seamount (n = 36) and east Equatorial Atlantic (n = 439). Solitary corals are shown in red and colonial corals are shown in black. Histograms show 2000-year bins. Error bars (2*s*) are shown in bottom panels. Top labels indicate MIS periods (1–6) and red shading marks MIS 5, 3 and 1.

BP, (iii) 32 to 12 kyr BP, and (iv) recent. The two oldest corals at Tropic Seamount (142 and 148 kyr BP) are from MIS 6 (Fig. 2). Over the subsequent ~100 kyr, cold-water corals remained sparse with only two coral samples dated at 82 kyr BP (colonial) and 56 kyr BP (solitary). A significant increase in coral abundance began at the end of MIS 3 (~32 kyr BP) and extended to the beginning of the Younger Dryas (YD; 13 to 11.7 kyr BP), with a transient peak (n = 11) during the Last Glacial Maximum (LGM, 22 to 18 kyr BP; Fig. 3). However, there are no corals recorded from 29 to 24.5 kyr BP (coincident with Heinrich Stadial 2, HS2) nor from 18 to 15.5 kyr BP (coincident with Heinrich Stadial 1 (18–14.7 kyr BP, HS1); Fig. 3). Next, there is a gap of ~12.5 kyr throughout the mid-YD and Holocene, including the last African Humid Period (8.2–5.5 kyr BP; Adkins et al., 2006), followed by the occurrence of four recent samples younger than 0.2 kyr BP (Fig. 3).

4.2.3. *East Equatorial Atlantic sites*

In addition to the corals dated in this study (n = 439), 92 previously published ages from the east Equatorial Atlantic are included in this discussion (Chen et al., 2015, 2016, 2020; Mangini et al., 1998). Considered together, the full dataset includes ages that range from 147 kyr BP to present (Fig. 2), and most of the corals are solitary (n = 503, with 28 colonial specimens). Solitary corals are found in this region throughout the last 147 kyr, except for the interval 120 to 95 kyr BP, while there are only three instances of colonial corals dated older than 17 kyr BP: at 146 kyr BP, 140 kyr BP, and 49 kyr BP (Fig. 2 and Fig. S4).

The occurrence of solitary corals in the Equatorial Atlantic is semi-continuous from 95 kyr BP, with increasing abundance from 50 kyr BP and a distinct peak between 16 and 14 kyr BP (HS1 and B-A). The latter peak is also observed for colonial corals. Subsequently, both solitary and colonial coral populations show a decrease from 12 to 4 kyr BP, and a recovery after 4 kyr BP (Fig. 2). The east Equatorial Atlantic dataset is distributed across three locations (Fig. 1): Carter Seamount (total n = 363 ages; 307 new ages and 56 published); Knipovich Seamount (total n = 167 ages; 132 new ages and 35 published); and the mid-Atlantic ridge at 2300 m depth aged 14.1 kyr BP (total n = 1; 1 age published; Mangini et al., 1998). Corals from both Carter and Knipovich seamounts show peak abundance during the HS1 and the B-A transition, and after 4 kyr BP (Fig. 2 and Fig. S4). A notable observation is that there are very few corals reported between 8.5 kyr BP and 4 kyr BP during the last African Humid Period (Fig. 3).

Another feature observed in the east Equatorial Atlantic is an apparent deeper coral occurrence (below ~1600 m) during warm climatic phases (MIS 5, 3 and 1) as well as during mid-MIS 6 and the last deglaciation, contrasting with shallower occurrences during glacial intervals (MIS 6, 4 and 2, Fig. 3). Intriguingly, the "deepening" in coral occurrence down to ~2000 m during the last deglaciation occurs at the same time as an increase in depth range (1800 m–2600 m) of coral populations at seamounts in the Northwest Atlantic (Thiagarajan et al., 2013). However, given few sites with sampling across a wide depth range we do not make any further interpretations on depth distribution in this study.

5. Discussion

5.1. *North to south differences in coral occurrence across the Northeast Atlantic*

A key observation from previous publications in the Northeast Atlantic is the latitudinal difference in coral occurrences over time (Frank et al., 2011). Corals from low and mid latitudes flourished during glacial and deglacial periods, whereas corals from higher latitudes were abundant during warm climate intervals – expanding their northernmost extent to the Norwegian margin after the Younger Dryas (López Correa et al., 2012). Our new dataset allows us to explore whether this feature is also apparent across the wider basin, and for solitary coral species which are underrepresented in the fossil record of the Northeast continental margin. Our data show that open-ocean habitats also exhibit distinct differences between high (Reykjanes Ridge) and low latitudes (east Equatorial Atlantic and Tropic Seamount), with the same warm/cold periods see-saw pattern observed in shelf settings (Frank et al., 2011).

Open-ocean corals from the Reykjanes Ridge are typically found during warm climate intervals at MIS 5, 3 and 1. During MIS 5, these ages are similar to those from coral mounds from the Porcupine Seabight and Rockall Trough (Dorschel et al., 2007; Frank et al., 2009, 2011; van der Land et al., 2010, 2014; Wienberg et al., 2020). During MIS 3, however, solitary corals are present at Reykjanes Ridge (n = 13 from 55 to 35 kyr BP), while they are largely absent on the continental margin north of 45°N (Fig. 4) with the exception of one coral age at Porcupine Seabight (53 ka; Dorschel et al., 2007). After a gap of 20,000 years, coinciding with the LGM and early deglaciation, solitary and colonial

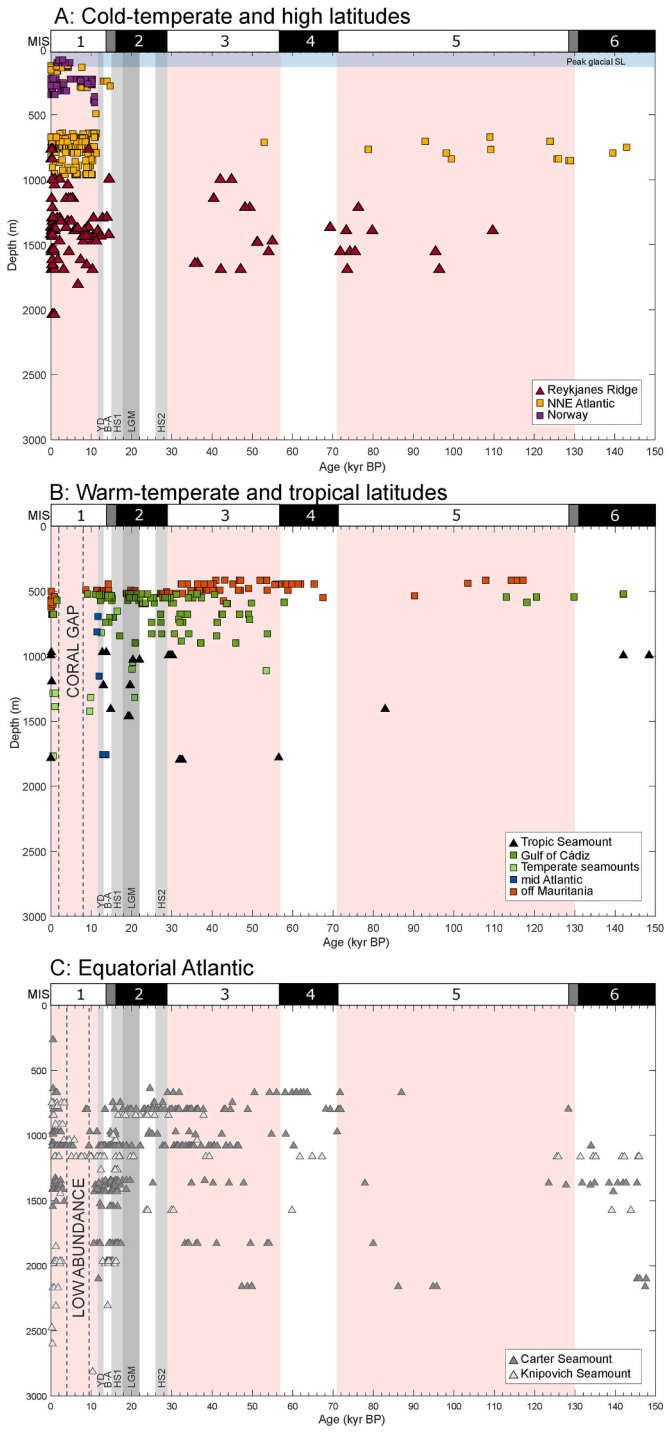

Fig. 3. Temporal depth distribution of cold-water corals from the Northeast Atlantic divided by region: (**A**) cold-temperate and high latitudes coral sites (note that Reykjanes Ridge samples are plotted as mean depths from maximum and minimum depths of dredges when on the seafloor); (**B**) tropical and warm-temperate coral sites; (**C**) east Equatorial Atlantic coral sites (see Table 1 and Fig. 1 for references). Square symbols represent previously published data and triangles represent coral sites from this study. Red shading indicates MIS 5, 3 and 1, and blue shading on panel A indicates the lowest glacial sea level (~130 m). Top labels indicate MIS periods (1–6), and glacial terminations 2 (130 kyr BP) and 1 (14 kyr BP) are indicated by dark grey bars. Shaded grey bars indicate climatic periods as follow: HS2 (Heinrich stadial 2, 28 to 24 kyr BP); LGM (Last Glacial Maximum, 22 to 18 kyr BP); HS1 (Heinrich stadial 1, 18 to 14.7 kyr BP); B-A (Bølling-Allerød, 14.7 to 13 kyr BP); YD (Younger Dryas, 13 to 11.7 kyr BP).

corals re-occur at Reykjanes Ridge during the B-A and show an increasing abundance through the Holocene (Fig. 4). Thus, the data suggest that during warm climatic phases prior to the Holocene (MIS 5, MIS 3 and B-A) the Reykjanes Ridge (~60°N) represented the northernmost limit of corals in the Northeast Atlantic (Figs. 4 and 5). During the Holocene corals re-occur at Porcupine Seabight and Rockall Trough, and as far north as the Norwegian margin (Fig. S5; Frank et al., 2011; Lindberg and Mienert, 2006; López Correa et al., 2012; Raddatz et al., 2016; Schröder-Ritzrau et al., 2005; Titschack et al., 2015; Wienberg et al., 2020) and at the Faroe Islands (Schröder-Ritzrau et al., 2005) pointing to a more northerly distribution.

Further south, corals from Tropic and east Equatorial Atlantic seamounts are more abundant during glacials (MIS 3 to 2; Figs. 2 and 4), similar to the Gulf of Cádiz (Wienberg et al., 2009, 2010), temperate latitude seamounts (Schröder-Ritzrau et al., 2003, 2005), and off Mauritania (Fig. 4; Eisele et al., 2011; Wienberg et al., 2018). All of these sites also share the following similarities: sparse or no coral occurrence during MIS 6 and 5, a reduction at the onset of the Holocene and a re-appearance in the last thousand years (Fig. 4). Of course, the sparse occurrence of corals during MIS 6 and 5 might be related to sampling limitations, for instance the use of short sediment cores on coral mounds.

Together, these observations from the combined coral dataset highlight basin-scale controls on both solitary and colonial corals from the continental shelf and slope as well as open-ocean habitats (e.g., seamounts and mid-ocean ridges). In the next sections we explore the controls in more detail.

5.2. Environmental drivers of coral distribution in the cold-temperate and high latitudes

The occurrence of coral mounds in cold, temperate latitudes has previously been linked to enhanced bottom water hydrodynamics as a main control of food and sediment fluxes (Frank et al., 2009, 2011; Wienberg et al., 2020). Additionally, corals from these locations and high latitudes were found to be situated within a narrow band of water density constraining the importance of oceanic circulation (De Mol et al., 2011; Dullo et al., 2008; Flögel et al., 2014). In this section, we first discuss the mechanisms associated with the higher (lower) coral abundance at these locations during warm (cold) climate intervals. Then, we compare the timing of coral occurrence at these sites and discuss the associated mechanisms during the last 15 kyr.

5.2.1. Comparison of warm and cold climatic intervals

During warm intervals, warm waters transported by the NAC reached the Nordic Seas and recirculated within the seas south of Iceland, and the Polar Front is thought to have shifted northward compared to colder intervals (Fig. 5; de Vernal et al., 2005; Pflaumann et al., 2003; Toucanne et al., 2021). This displacement would have diminished regional sea-ice formation, stimulating primary productivity and increasing food availability for benthic communities (Matul et al., 2018). Analogous to the modern day, the waters transported by the NAC would also have acted as an additional source of biomass through advection of phytoplankton towards the Nordic Seas and Arctic Ocean (Vernet et al., 2019). Therefore, we argue that these changes in oceanic circulation together with the associated increase in temperature and food availability would have affected coral communities, driving high coral abundances in the northern Northeast Atlantic during MIS 5 and 1 (Fig. 4; for discussion of MIS 1 see Section 5.2.2). During the MIS 3, a similar mechanism is expected to be associated with the occurrence of corals at Reykjanes Ridges. This is supported by evidence of a decrease in polar waters and an increase of temperate waters occurring south of Iceland during early and mid-MIS 3 (Bashirova et al., 2014). However, the contrasting low occurrence or absence of corals at Porcupine Seabight and the Rockall Trough point towards additional forcing, for instance hydrodynamic processes controlling food and sediment flux (Wienberg et al., 2020).

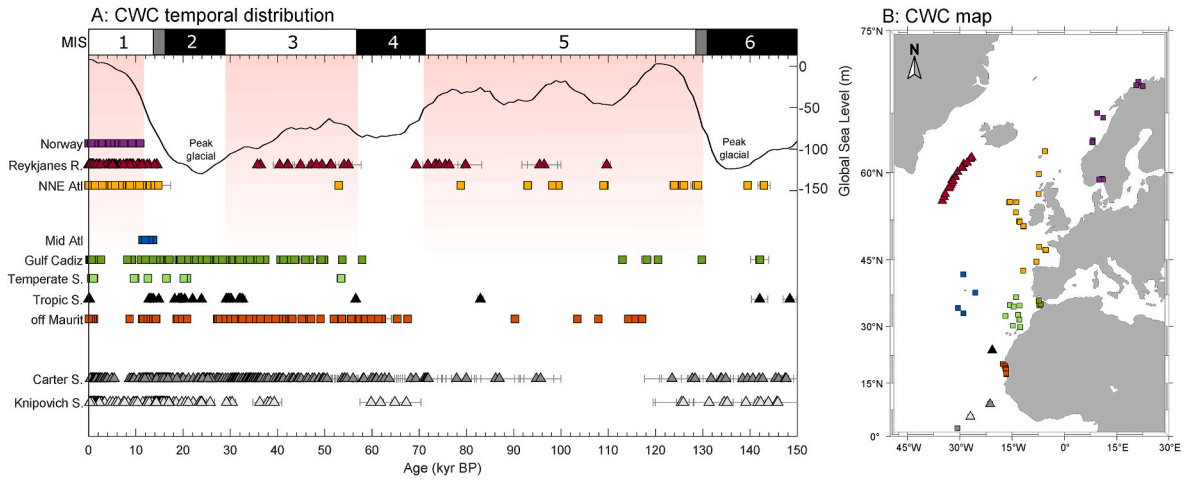

Fig. 4. (**A**) Compiled age distributions of cold-water corals from the Northeast Atlantic (see Table 1 and Fig. 1 for references) and global sea level reconstruction (Spratt and Lisiecki, 2016). Red shading indicates MIS 5, 3 and 1, coincident with intervals of abundant high latitude corals. Top labels indicate MIS periods (1–6), and glacial terminations 2 (130 kyr BP) and 1 (14 kyr BP) are indicated by dark grey bars. (**B**) Map of cold-water corals shown and colour matched with panel A. Square symbols represent previously published data and triangles represent coral sites from this study (Reykjanes Ridge, Tropic Seamount, Carter Seamount and Knipovich Seamount).

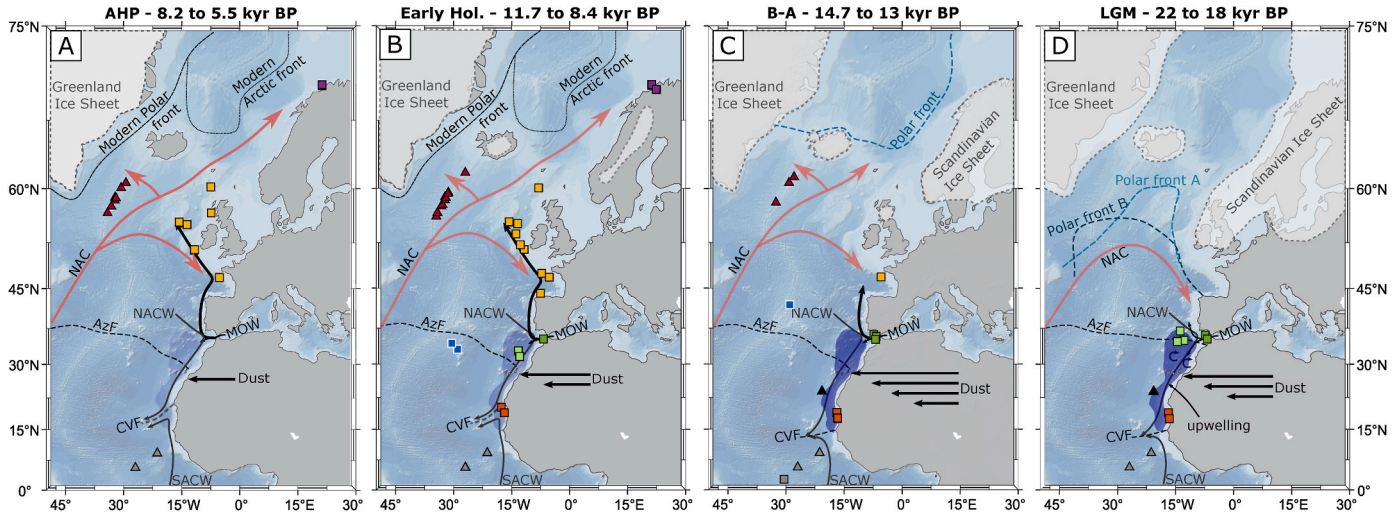

Fig. 5. Schematic representation of main mechanisms associated with cold-water coral distribution in the Northeast Atlantic Ocean at four time slices: (**A**) African Humid Period (AHP, 8.2 to 5.5 kyr BP), (**B**) early Holocene (11.7–8.4 kyr BP), (**C**) Bølling-Allerød (B-A, 14.7 to 13 kyr BP), and (**D**) Last Glacial Maximum (LGM, 22 to 18 kyr BP). Polar Front A and B (panel D) corresponds to reconstructions by Pflaumann et al. (2003) and de Vernal et al. (2005) respectively; and Polar Front (panel C) follows Xiao et al. (2017). Approximate position of ice sheets and Polar and Arctic Fronts (panels B and A) after (De Vernal et al., 2005; Hughes et al., 2016; Pflaumann et al., 2003). Schematic dust fluxes are according to (McGee et al., 2013). Coastal and frontal upwelling at the Northwest African margin are shown with the shaded blue area (Bradtmiller et al., 2016; Romero et al., 2008; Zarriess and Mackensen, 2010). Main pathway of Mediterranean Overflow Water (MOW) is indicated by black arrows exiting the Strait of Gibraltar (Rogerson et al., 2005). The North Atlantic Current (NAC) is indicated by red arrows (Matul et al., 2018; Thornalley et al., 2011). Inferred positions of North Atlantic Central Water (NACW) and South Atlantic Central Water (SACW) are indicated by dark grey arrows (Wienberg et al., 2018). Cape Verde (CVF) and Azores (AzF) frontal positions are after (Romero et al., 2008; Wienberg et al., 2010, 2018).

The opposite mechanism likely explains the sparseness of corals in cold-temperate and high latitude locations during glacial intervals (e.g. MIS 4 and 2, Fig. 4). During these cold periods, primary productivity was likely limited by enhanced sea-ice cover following a southward shift in the Polar Front (Fig. 5; Löfverström et al., 2014). This shift would have been particularly important at latitudes north of 45°N when the NAC is thought to have shifted towards to a nearly zonal position around 40°N - 50°N (Fig. 5; Eynaud et al., 2009). Supporting this frontal shift, reconstructions of sea surface temperature and salinity south of Iceland suggest a large winter sea-ice expansion during the LGM (Thornalley et al., 2011), paired with the absence of corals at Reykjanes Ridge (Fig. 5). In summary, coral occurrences from cold-temperate and high latitudes have been responding to intervals of increased food availability paced by warm climate intervals.

5.2.2. *The last 15 kyr*

During the last 15 kyr corals re-occur at Reykjanes Ridge during the interstadial B-A, followed by a re-aggradation of coral mounds at Porcupine Seabight and Rockall Trough, and a northward migration of corals up to the Norwegian shelf (Bonneau et al., 2018; Dorschel et al., 2007; Douarin et al., 2013; Eisele et al., 2008; Frank et al., 2004, 2009, 2011; Mienis et al., 2009; Schröder-Ritzrau et al., 2003, 2005; van der Land et al., 2010, 2014; Victorero et al., 2016; Wienberg et al., 2020).

The re-occurrence of cold-water corals (both solitary and colonial) at Reykjanes Ridge during the B-A (Fig. 4 and Fig. S5) parallels a regional increase of organic matter (high abundance of benthic foraminifera

Cassidulina teretis; Matul et al., 2018) and an increase in the export of dense, oxygen-rich overflow waters from the Nordic Seas (1179 m; Ezat et al., 2017). These findings suggest that the coral community at Reykjanes Ridge benefited from the enhanced food supply and likely enhanced oxygenation of subsurface waters promoted by the increased flow of the deep waters.

The timing of the coral re-occurrence at Reykjanes Ridge around 14.5 kyr BP aligns with an increase in abundance of corals in the Bay of Biscay (Fig. 5; note there are only 12 ages available from the Bay of Biscay; De Mol et al., 2011; Schröder-Ritzrau et al., 2003), however, coral mound formation at Porcupine Seabight and Rockall Trough remained inactive until 11.3 kyr BP (Dorschel et al., 2007; Frank et al., 2009, 2011; van der Land et al., 2010, 2014; Wienberg et al., 2020). One potential reason put forth for this inactivity is related to sluggish bottom currents (Wienberg et al., 2020). Later on, during the onset of the Holocene, it has been suggested that the location of the coral mounds within a highly dynamic transition zone may have promoted hydrodynamic conditions favourable to coral growth, such as enhanced food and sediment supply (Fig. 5; Wienberg et al., 2020). This could have been a result of the invigoration of the MOW, and the establishment of its modern depth and intensity flow pattern (Rogerson et al., 2005; Wienberg et al., 2020).

Further north, the onset of coral growth at the Norwegian shelf occurred at 10.9 kyr BP, around 400 yr after re-growth at coral mounds in the Porcupine Seabight and Rockall Trough suggesting a rapid climate driven coral migration (Frank et al., 2011; López Correa et al., 2012). The start of the Norwegian coral ecosystems is contemporaneous with the establishment of modern-like warm climatic conditions and oceanographic patterns (López Correa et al., 2012). Additionally, evidence based on genetic traits of modern coral communities has been used to suggest that coral larvae were coming from the Mediterranean Sea and out into the British Isles and Norwegian shelf at the onset of the Holocene (Henry et al., 2014). This evidence has been supported by Boavida et al. (2019) who demonstrated a northward expansion of cold-water corals after the end of the last glacial from the Mediterranean Sea to the North Atlantic, with a nearly homogenised genetic signature of *Desmophyllum pertusum* (*Lophelia pertusa*) from the Bay of Biscay to the Iceland margin. Overall, the overflow waters from the Mediterranean Sea may play an important role in the Northeast Atlantic coral community by influencing regional hydrodynamics, food supply and larvae dispersion.

5.3. Environmental drivers of coral distribution in the low and mid-latitudes

The temporal distribution of corals from low and mid-latitudes in the Northeast Atlantic contrasts with the distribution of corals further north by having the most prolific growth during the last glacial interval, and a strong decrease in abundance at the onset of the Holocene. Previous studies attributed this pattern to productivity, shifts in oceanographic fronts, and hydrological conditions such as temperature and dissolved oxygen (Eisele et al., 2011; Frank et al., 2011; Wienberg et al., 2009, 2010, 2018). The similar occurrence pattern observed for corals from the east Equatorial Atlantic and Tropic Seamount point towards basin-scale mechanisms paced by climatic shifts. In this section we present a discussion of the mechanisms associated with this coral pattern during four time intervals: the last glaciation, HS1, early-Holocene, and African Humid Period and present.

5.3.1. Last glacial interval and LGM

During the onset of the MIS 4, an increase in coral population in the east Equatorial Atlantic (Fig. 2 and Fig. S4) is associated with higher total organic carbon (TOC) and biogenic opal compared to interglacials (Wagner, 2000). At the same time, coral mounds off Mauritania re-initiated as a response to an increased in food supply (Eisele et al., 2011; Portilho-Ramos et al., 2022; Wienberg et al., 2018). In addition to productivity, Wienberg et al. (2018) suggests that a southward displacement of Cape Verde Frontal Zone would have placed these coral mounds within the oxygen-rich North Atlantic Central Water, promoting favourable conditions for coral growth.

During the LGM and deglaciation, high coral abundances at Gulf of Cádiz, temperate latitude seamounts, Tropic Seamount and Mauritania margin occur at the same time as aeolian fluxes were up to two times higher than the present (Fig. 6; McGee et al., 2013; Middleton et al., 2018; Rowland et al., 2021). The high aeolian fluxes and the increase in coastal and frontal upwelling (Adkins et al., 2006; Romero et al., 2008) resulted in high productivity off Northwest Africa (Bradtmiller et al., 2016) and in the Gulf of Cádiz (Wienberg et al., 2010) providing additional food resources to corals. The contemporaneous high coral abundance at Tropic Seamount suggests that these organic-rich waters reached the offshore location of the seamount, increasing food supply and sustaining favourable conditions for corals (Fig. 5). Contrasting to this prolific coral growth, corals from the east Equatorial Atlantic show a reduced occurrence. In fact, there was a reduction of the organic matter export to the sea floor (e.g., low TOC) in the Equatorial Atlantic during the LGM (Zarriess and Mackensen, 2010), further demonstrating the strong link between productivity and east Equatorial Atlantic corals.

5.3.2. Heinrich Stadial 1

While productivity seems to be the dominant driver of coral abundance (Section 5.3.1), a different mechanism may have dominated during Heinrich Stadial 1. At this time, reconstructions of productivity from the Equatorial Atlantic and NW African margin show a pronounced increase (Bradtmiller et al., 2016; McKay et al., 2014; Romero et al., 2008; Zarriess and Mackensen, 2010), which occurred during the most pronounced coral abundance peak in the east Equatorial Atlantic (Fig. 6). By contrast, corals were absent at the Mauritanian margin and Tropic Seamount (Fig. 6 and Fig. S5).

During HS1, the presence of the oxygen-poor South Atlantic Central Water on the Mauritanian continental shelf and slope may have reduced coral mound growth (Wienberg et al., 2018). A similar pattern of coral growth observed at our new Tropic Seamount site suggests that deoxygenation of the water column at this time may also have occurred further offshore and at deeper depths (between 1000 m and 1500 m in contrast with corals off Mauritania at ~500 m). It is unlikely that the same mechanism (e.g., coral site location within the central waters) would explain this lowering in seawater oxygen content at Tropic Seamount. Instead, we argue that the high input of organic matter onto the sea floor may have promoted low benthic oxygen conditions. In agreement with this idea, an increase in abundance of local benthic foraminifera tolerant to low oxygen is described at the continental slope (~2500 m) off Mauritania during the HS1 (McKay et al., 2014).

5.3.3. Early-holocene

During the early-Holocene, a pronounced decrease in coral population is observed in the east Equatorial Atlantic, Tropic Seamount, Gulf of Cádiz, temperate latitude seamounts and Mauritania margin (Fig. 6). In fact, the abundance pattern of corals in the east Equatorial Atlantic mimics the pattern of dust fluxes and productivity, with a coral gap of more than 12 thousand years at Tropic Seamount coeval with low values for these two parameters (Fig. 6). The reduced dust fluxes during the early Holocene (e.g., McGee et al., 2013; Middleton et al., 2018; Rowland et al., 2021) could have directly impacted primary productivity decreasing "iron fertilization" of surface ocean (Mark Moore et al., 2009; Wienberg et al., 2010). Furthermore, the associated weakened trade winds are thought to have reduced coastal upwelling intensity as suggested by low opal flux and organic carbon observed at the entire Northwest African margin between 19°N and 27°N (Bradtmiller et al., 2016). In addition, diatom assemblages from the continental slope off Mauritania also indicate low productivity during the Holocene in agreement with a reduced coastal upwelling (McKay et al., 2014). Recently, Portilho-Ramos et al. (2022) demonstrated that coral

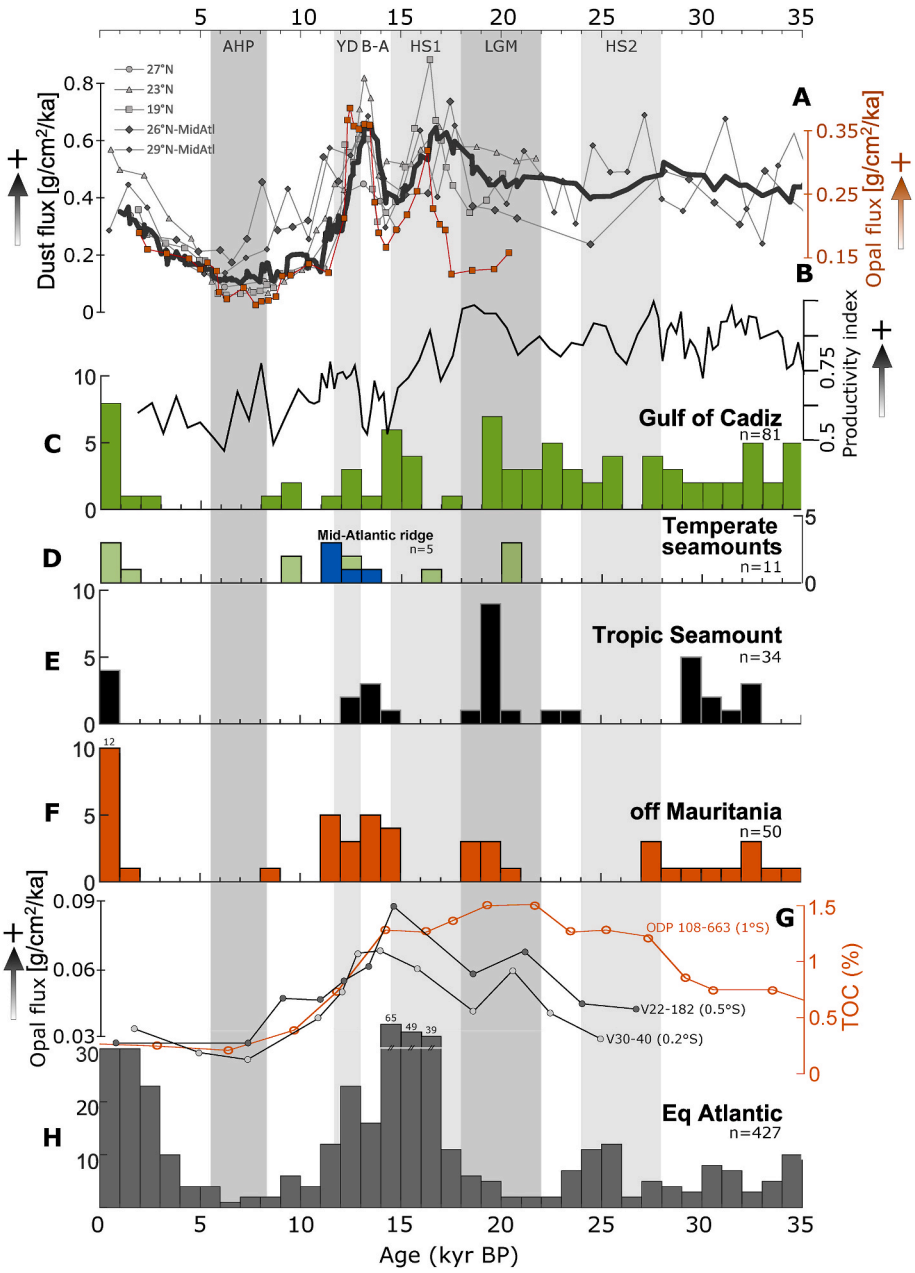

Fig. 6. Age distribution of cold-water corals from the tropical and central Northeast Atlantic and environmental proxies from the past 35 kyr BP. (**A**) Compilation of dust fluxes from Northwest Africa from cores OC437-7 GC68 (19°N, scaled down 6 times), GC49 (23°N), GC37 (27°N) (McGee et al., 2013), KN207-2 GGC3 (26°N), GGC6 (29°N) (Middleton et al., 2018), black line corresponds to the 6-point moving average. Opal flux from the Mauritanian margin (orange symbols, same core as dust record at 19°N; Bradtmiller et al., 2016). (**B**) Productivity index at Gulf of Cádiz based on planktonic foraminiferal assemblages from core GeoB9064 (Wienberg et al., 2010). (**C**) Histogram of cold-water corals of Gulf of Cádiz (green; Dubois-Dauphin et al., 2016; Frank et al., 2011; Schröder-Ritzrau et al., 2005, 2003; Wienberg et al., 2010, 2009). (**D**) Histogram of cold-water corals from seamounts at temperate latitudes (light green; Schröder-Ritzrau et al., 2005, 2003) and mid-Atlantic (blue; Adkins et al., 1998; Eltgroth et al., 2006; Schröder-Ritzrau et al., 2005, 2003). (**E**) Histogram of cold-water corals from Tropic Seamount (this study). (**F**) Histogram of cold-water corals from the Mauritanian margin (Eisele et al., 2011; Wienberg et al., 2018). (**G**) Opal fluxes from Equatorial Atlantic from cores V22–182 and V30-40 (Bradtmiller et al., 2007) and total organic carbon (TOC) from core ODP 108–663 (Wagner, 2000). (**H**) Histogram of cold-water corals from east Equatorial Atlantic (this study; Chen et al., 2020, 2016, 2015; Mangini et al., 1998). Histograms show number of corals dated and total number of samples (n). Shaded bars indicate climatic periods as follow: LGM (Last Glacial Maximum, 22 to 18 kyr BP); HS1 (Heinrich stadial 1, 18 to 14.7 kyr BP); B-A (Bølling-Allerød, 14.7 to 13 kyr BP); YD (Younger Dryas, 13 to 11.7 kyr BP); AHP (African Humid Period, 8.2 to 5.5 kyr BP). For site location references see Fig. S1.

occurrences on the Mauritania margin and Gulf of Cádiz are strongly associated with food supply. They attributed the lack of coral occurrence during the onset of the Holocene to a decrease in organic matter flux and weakened bottom currents (Portilho-Ramos et al., 2022).

In addition to coastal upwelling, the absence of corals on the upper slope off Mauritania in the Holocene has been attributed to the presence of the oxygen-poor South Atlantic Central Water due to the northward shift of the Cape Verde Frontal Zone (Fig. 5). At the same time, the southward position of the Azores Front (~30°N; Fig. 5) displaced the higher productivity area away from the Gulf of Cádiz, thus decreasing food supply (Wienberg et al., 2010). In addition to these oceanographic and hydrological changes, warmer seawater temperatures after the Younger Dryas was thought to be a potential extra stressor for the local coral community (Wienberg et al., 2010, 2018). However, the recent Mauritania margin and Gulf of Cádiz study suggests that temperature played little role in coral demise during the Holocene (Portilho-Ramos et al., 2022).

5.3.4. *African Humid Period and present*

In the east Equatorial Atlantic, the coral population sharply decreases from the onset of the Holocene until it reaches the lowest coral abundance during the last African Humid Period (Fig. 6). During this interval, African vegetation and precipitation combined with weaker trade winds led to low dust flux and a pronounced decrease in coastal upwelling (Fig. 5; Adkins et al., 2006; Bradtmiller et al., 2016). Similarly, corals are absent on the Mauritania margin, Tropic Seamount, Gulf of Cádiz and temperate seamounts throughout the last African Humid Period (Fig. 5). Our data indicate that the influence of these changes in productivity extended across the basin, and that this interval, together with the shifts on oceanographic fronts and hydrological conditions (Section 5.3.3), represents the most unfavourable conditions for coral growth at mid to low latitudes within the Holocene.

The modern coral communities at all mid to low latitude sites are characterized by a patchy occurrence and low numbers which seems to be controlled by specific and local conditions (e.g., enhanced hydrodynamics supplying food and oxygen), differing considerably from the

thriving glacial/deglacial reefs. For instance, modern corals at Tropic Seamount are mostly observed on the eastern and western flanks, where higher current and energy may increase food supply. And at the Mauritanian margin, late-Holocene corals are observed exclusively within canyons, where episodic events can deliver food and well-oxygenated surface waters into the deep (Wienberg et al., 2018). In summary, productivity seems to be the main driver of coral abundance across the region. Other parameters as oxygen concentration and temperature however may still act as stressors controlling coral growth, with local factors also influencing coral distributions.

6. Conclusions

We have combined >600 new U-series dates of fossil scleractinian cold-water corals from the tropical and high latitude Northeast Atlantic Ocean with previous published data to yield a database of over 1300 coral dates. Systematic analysis of the temporal distribution of the coral population shows that the corals are affected by basin wide climate-driven oceanographic and hydrologic change. We demonstrate that the timing of colonial and solitary cold-water coral occurrence is similar, suggesting similar survival needs. Furthermore, we reveal an analogous temporal distribution between coral population from continental shelf, slope and open-sea regime. This extensive database includes equatorial regions, where corals show contrasting distribution patterns compared to the high latitude Northeast Atlantic.

Sites in the cold-temperate and high latitude Northeast Atlantic reveal peak coral occurrences during warm climate intervals over the past 150 kyr BP, and the Reykjanes Ridge (~60°N) represents the known biogeographical limit of cold-water corals during MIS 5 and 3. Regionally, cold-water coral success is thought to be controlled by oceanic dynamics, especially the inflow of warm Atlantic waters by NAC, the Polar Front position, and the influence of MOW at coral mounds on continental margins, all mechanisms associated with food and sediment supply. During the early Holocene, the biogeographical limit of cold-water corals expands from Reykjanes Ridge (~60°N) to the Norwegian shelf (~70°N), a time when full interglacial conditions and modern-like circulation patterns were established.

A contrasting pattern is observed in the low and mid latitude Northeast Atlantic, where corals show prolific growth during the last glacial and deglacial intervals, and a pronounced decline during the early and mid-Holocene. This finding had been based mainly on observations of corals mounds on the continental slope off Northwest Africa (Eisele et al., 2011; Frank et al., 2011; Wienberg et al., 2010, 2018). Our new and extensive record of Equatorial Atlantic corals however confirms the broad scale of this pattern. We find the glacial/deglacial large scale coral occurrence is linked to surface water productivity driven by enhanced dust fertilization and stronger upwelling systems. Additionally, water column oxygenation is shown as an important factor to coral growth mainly driven by frontal zone positions or organic matter remineralization. The collapse of central and equatorial Northeast Atlantic coral populations during the Holocene occurs with a drastic decrease in wind strength and aridity in Africa. Moreover, lower concentrations of dissolved oxygen and higher temperatures, may have acted as additional stressors to corals inhabiting the continental slope.

Past climate-driven shifts in cold-water corals towards higher latitudes during warm intervals mean that future warming and associated sea ice reduction, if moderate and gradual, may open new niches for corals. However, the fast rates of warming have already impacted key regions of the ocean declining primary productivity (Capuzzo et al., 2018) and oxygen concentration (Santos et al., 2016). These factors combined with ocean acidification/aragonite saturation horizon shoaling (Carvalho-Borges et al., 2018; Guinotte et al., 2006) will doubtless present challenges to calcifying organisms with unknown consequences for the future of cold-water corals and the important habitats that they engineer.

Declaration of competing interest

The authors declare that they have no known competing financial interests or personal relationships that could have appeared to influence the work reported in this paper.

Data availability

The new data and compilation reported in this paper are archived in Pangaea (https://doi.pangaea.de/10.1594/PANGAEA.945280).

Acknowledgements

We acknowledge the crew and researchers on board the research cruises JC142 (Tropic Seamount in 2016; project 'MarineE-tech'; grants NE/M011186/1, awarded to B. Murton and NE/M011151/1, awarded to P. Lusty), JC094 (Equatorial Atlantic in 2013) and CE08-06 (Reykjanes Ridge in 2008) who obtained the samples for this study. We thank Christopher Coath, Carolyn Taylor and Yun-Ju Sun for their help with laboratory work. We thank the editors, Sophia Hines, and two other reviewers for their comments which considerably improved this manuscript. Funding was provided by NERC grants awarded to L.F.R. (NE/S001743/1 and NE/R005117/1) and by Schlumberger Foundation who provided the PhD scholarship "Faculty for the Future Fellowship". M.V.K. acknowledges the support from the São Paulo Research Foundation (FAPESP #2017/50229-5) and from the National Council for Scientific and Technological Development (CNPq #301436/2018-5).

Appendix A. Supplementary data

Supplementary data to this article can be found online at https://doi.org/10.1016/j.dsr.2022.103892.

References

Adkins, J., deMenocal, P., Eshel, G., 2006. The "African humid period" and the record of marine upwelling from excess ^{230}Th in Ocean Drilling Program Hole 658C. Paleoceanography 21, 1–14. https://doi.org/10.1029/2005PA001200.

Adkins, J.F., Cheng, H., Boyle, E.A., Druffel, E.R.M., Edwards, R.L., 1998. Deep-sea coral evidence for rapid change in ventilation of the deep North Atlantic 15,400 Years ago. Science 80–, 725–728. https://doi.org/10.1126/science.280.5364.725.

Andersen, M.B., Stirling, C.H., Zimmermann, B., Halliday, A.N., 2010. Precise determination of the open ocean ^{234}U/^{238}U composition. G-cubed 11. https://doi.org/10.1029/2010GC003318.

Auro, M.E., Robinson, L.F., Burke, A., Bradtmiller, L.I., Fleisher, M.Q., Anderson, R.F., 2012. Improvements to 232-thorium, 230-thorium, and 231-protactinium analysis in seawater arising from GEOTRACES intercalibration. Limnol Oceanogr. Methods 10, 464–474. https://doi.org/10.4319/lom.2012.10.464.

Bashirova, L.D., Kandiano, E.S., Sivkov, V.V., Bauch, H.A., 2014. Migrations of the North Atlantic Polar front during the last 300 ka: evidence from planktic foraminiferal data. Oceanology 54, 798–807. https://doi.org/10.1134/S0001437014060010.

Blois, J.L., Zarnetske, P.L., Fitzpatrick, M.C., Finnegan, S., 2013. Climate change and the past, present, and future of biotic interactions. Science 341, 499–504. https://doi.org/10.1126/science.1237184.

Boavida, J., Becheler, R., Choquet, M., Frank, N., Taviani, M., Bourillet, J., Meistertzheim, A., Grehan, A., Savini, A., Arnaud-Haond, S., 2019. Out of the Mediterranean? Post-glacial colonization pathways varied among cold-water coral species. J. Biogeogr. 46, 915–931. https://doi.org/10.1111/jbi.13570.

Bonneau, L., Colin, C., Pons-Branchu, E., Mienis, F., Tisnérat-Laborde, N., Blamart, D., Elliot, M., Collart, T., Frank, N., Foliot, L., Douville, E., 2018. Imprint of Holocene climate variability on cold-water coral reef growth at the SW Rockall Trough margin, NE atlantic. G-cubed 19, 2437–2452. https://doi.org/10.1029/2018GC007502.

Bradtmiller, L.I., Anderson, R.F., Fleisher, M.Q., Burckle, L.H., 2007. Opal burial in the equatorial Atlantic Ocean over the last 30 ka: implications for glacial-interglacial changes in the ocean silicon cycle. Paleoceanography 22. https://doi.org/10.1029/2007PA001443.

Bradtmiller, L.I., McGee, D., Awalt, M., Evers, J., Yerxa, H., Kinsley, C.W., DeMenocal, P. B., 2016. Changes in biological productivity along the northwest African margin over the past 20,000 years. Paleoceanography 31, 185–202. https://doi.org/10.1002/2015PA002862.

Burke, A., Robinson, L.F., 2012. The Southern Ocean's role in carbon exchange during the last deglaciation. Science 335, 557–562. https://doi.org/10.1126/science.1208163.

Canadell, J.G., Monteiro, P.M.S., Costa, M.H., Cotrim da Cunha, L., Cox, P.M., Eliseev, A. V., Henson, S., Ishii, M., Jaccard, S., Koven, C., Lohila, A., Patra, P.K., Piao, S.,

Rogelj, J., Syampungani, S., Zaehle, S., Zickfeld, K., 2021. Global carbon and other biogeochemical cycles and feedbacks. In: Zhai, P., Pirani, A., Connors, S.L., Péan, C., Berger, S., Caud, N., Chen, Y., Goldfarb, L., Gomis, M.I., Huang, M., Leitzell, K., Lonnoy, E., Matthews, J.B.R., Maycock, T.K., Waterfield, T., Yelekçi, O., Yu, R., Zhou, B. (Eds.), Climate Change 2021: the Physical Science Basis. Contribution of Working Group I to the Sixth Assessment Report of the Intergovernmental Panel on Climate Change [Masson-Delmotte, V. Cambridge University Press, Cambridge, United Kingdom and New York, NY, USA, pp. 673–816. https://doi.org/10.1017/9781009157896.007.

Capuzzo, E., Lynam, C.P., Barry, J., Stephens, D., Forster, R.M., Greenwood, N., McQuatters-Gollop, A., Silva, T., van Leeuwen, S.M., Engelhard, G.H., 2018. A decline in primary production in the North Sea over 25 years, associated with reductions in zooplankton abundance and fish stock recruitment. Global Change Biol. 24, e352–e364. https://doi.org/10.1111/gcb.13916.

Carvalho-Borges, M. de, Orselli, I.B.M., Ferreira, M.L. de C., Kerr, R., 2018. Seawater acidification and anthropogenic carbon distribution on the continental shelf and slope of the western South Atlantic Ocean. J. Mar. Syst. 187, 62–81. https://doi.org/10.1016/j.jmarsys.2018.06.008.

Chen, T., Robinson, L.F., Beasley, M.P., Claxton, L.M., Andersen, M.B., Gregoire, L.J., Wadham, J., Fornari, D.J., Harpp, K.S., 2016. Ocean mixing and ice-sheet control of seawater $^{234}U/^{238}U$ during the last deglaciation. Science 354, 626–629. https://doi.org/10.1126/science.aag1015.

Chen, T., Robinson, L.F., Burke, A., Claxton, L., Hain, M.P., Li, T., Rae, J.W.B., Stewart, J., Knowles, T.D.J., Fornari, D.J., Harpp, K.S., 2020. Persistently well-ventilated intermediate-depth ocean through the last deglaciation. Nat. Geosci. 13, 733–738. https://doi.org/10.1038/s41561-020-0638-6.

Chen, T., Robinson, L.F., Burke, A., Southon, J., Spooner, P., Morris, P.J., Ng, H.C., 2015. Synchronous centennial abrupt events in the ocean and atmosphere during the last deglaciation. Science 349, 1537–1541. https://doi.org/10.1126/science.aac6159.

Cheng, H., Adkins, J., Edwards, R.L., Boyle, E.A., 2000. U-Th dating of deep-sea corals. Geochem. Cosmochim. Acta 64, 2401–2416. https://doi.org/10.1016/S0016-7037(99)00422-6.

Davies, A.J., Guinotte, J.M., 2011. Global habitat suitability for framework-forming cold-water corals. PLoS One 6, e18483. https://doi.org/10.1371/journal.pone.0018483.

de Carvalho Ferreira, M.L., Kerr, R., 2017. Source water distribution and quantification of North atlantic deep water and antarctic bottom water in the Atlantic Ocean. Prog. Oceanogr. 153, 66–83. https://doi.org/10.1016/j.pocean.2017.04.003.

De Mol, L., Van Rooij, D., Pirlet, H., Greinert, J., Frank, N., Quemmerais, F., Henriet, J.-P., 2011. Cold-water coral habitats in the penmarc'h and guilvinec canyons (Bay of Biscay): deep-water versus shallow-water settings. Mar. Geol. 282, 40–52. https://doi.org/10.1016/j.margeo.2010.04.011.

de Vernal, A., Eynaud, F., Henry, M., Hillaire-Marcel, C., Londeix, L., Mangin, S., Matthiessen, J., Marret, F., Radi, T., Rochon, A., Solignac, S., Turon, J.L., 2005. Reconstruction of sea-surface conditions at middle to high latitudes of the Northern Hemisphere during the Last Glacial Maximum (LGM) based on dinoflagellate cyst assemblages. Quat. Sci. Rev. 24, 897–924. https://doi.org/10.1016/j.quascirev.2004.06.014.

Dodds, L.A., Roberts, J.M., Taylor, A.C., Marubini, F., 2007. Metabolic tolerance of the cold-water coral Lophelia pertusa (Scleractinia) to temperature and dissolved oxygen change. J. Exp. Mar. Biol. Ecol. 349, 205–214. https://doi.org/10.1016/j.jembe.2007.05.013.

Dorschel, B., Hebbeln, D., Rüggeberg, A., Dullo, C., 2007. Carbonate budget of a cold-water coral carbonate mound: propeller Mound, Porcupine Seabight. Int. J. Earth Sci. 96, 73–83. https://doi.org/10.1007/s00531-005-0493-0.

Dorschel, B., Hebbeln, D., Rüggeberg, A., Dullo, W.C., Freiwald, A., 2005. Growth and erosion of a cold-water coral covered carbonate mound in the Northeast Atlantic during the Late Pleistocene and Holocene. Earth Planet Sci. Lett. 233, 33–44. https://doi.org/10.1016/j.epsl.2005.01.035.

Douarin, M., Elliot, M., Noble, S.R., Sinclair, D., Henry, L.-A., Long, D., Moreton, S.G., Murray Roberts, J., 2013. Growth of north-east Atlantic cold-water coral reefs and mounds during the Holocene: a high resolution U-series and ^{14}C chronology. Earth Planet Sci. Lett. 375, 176–187. https://doi.org/10.1016/j.epsl.2013.05.023.

Dubois-Dauphin, Q., Bonneau, L., Colin, C., Montero-Serrano, J.-C., Montagna, P., Blamart, D., Hebbeln, D., Van Rooij, D., Pons-Branchu, E., Hemsing, F., Wefing, A.-M., Frank, N., 2016. South Atlantic intermediate water advances into the North-east Atlantic with reduced Atlantic meridional overturning circulation during the last glacial period. G-cubed 17, 2336–2353. https://doi.org/10.1002/2016GC006281.

Dullo, W.-C., Flögel, S., Rüggeberg, A., 2008. Cold-water coral growth in relation to the hydrography of the Celtic and Nordic European continental margin. Mar. Ecol. Prog. Ser. 371, 165–176. https://doi.org/10.3354/meps07623.

Eisele, M., Frank, N., Wienberg, C., Hebbeln, D., López Correa, M., Douville, E., Freiwald, A., 2011. Productivity controlled cold-water coral growth periods during the last glacial off Mauritania. Mar. Geol. 280, 143–149. https://doi.org/10.1016/j.margeo.2010.12.007.

Eisele, M., Hebbeln, D., Wienberg, C., 2008. Growth history of a cold-water coral covered carbonate mound — galway Mound, Porcupine Seabight, NE-Atlantic. Mar. Geol. 253, 160–169. https://doi.org/10.1016/j.margeo.2008.05.006.

Eltgroth, S.F., Adkins, J.F., Robinson, L.F., Southon, J., Kashgarian, M., 2006. A deep-sea coral record of North Atlantic radiocarbon through the Younger Dryas: evidence for intermediate water/deepwater reorganization. Paleoceanography 21, 1–12. https://doi.org/10.1029/2005PA001192.

Eynaud, F., De Abreu, L., Voelker, A., Schönfeld, J., Salgueiro, E., Turon, J.L., Penaud, A., Toucanne, S., Naughton, F., Sánchez Goñi, M.F., Malaizé, B., Cacho, I., 2009. Position of the Polar Front along the western Iberian margin during key cold episodes of the last 45 ka. G-cubed 10. https://doi.org/10.1029/2009GC002398.

Ezat, M.M., Rasmussen, T.L., Thornalley, D.J.R.R., Olsen, J., Skinner, L.C., Hönisch, B., Groeneveld, J., 2017. Ventilation history of Nordic Seas overflows during the last (de)glacial period revealed by species-specific benthic foraminiferal ^{14}C dates. Paleoceanography 32, 172–181. https://doi.org/10.1002/2016PA003053.

Flögel, S., Dullo, W.-C., Pfannkuche, O., Kiriakoulakis, K., Rüggeberg, A., 2014. Geochemical and physical constraints for the occurrence of living cold-water corals. Deep. Res. Part II 99, 19–26. https://doi.org/10.1016/j.dsr2.2013.06.006.

Foubert, A., Depreiter, D., Beck, T., Maignien, L., Pannemans, B., Frank, N., Blamart, D., Henriet, J., 2008. Carbonate mounds in a mud volcano province off north-west Morocco: key to processes and controls. Mar. Geol. 248, 74–96. https://doi.org/10.1016/j.margeo.2007.10.012.

Frank, N., Freiwald, A., Correa, M.L., Wienberg, C., Eisele, M., Hebbeln, D., Van Rooij, D., Henriet, J.-P., Colin, C., van Weering, T., de Haas, H., Buhl-Mortensen, P., Roberts, J.M., De Mol, B., Douville, E., Blamart, D., Hatte, C., 2011. Northeastern Atlantic cold-water coral reefs and climate. Geology 39, 743–746. https://doi.org/10.1130/G31825.1.

Frank, N., Paterne, M., Ayliffe, L., van Weering, T., Henriet, J.-P., Blamart, D., 2004. Eastern North Atlantic deep-sea corals: tracing upper intermediate water $\Delta^{14}C$ during the Holocene. Earth Planet Sci. Lett. 219, 297–309. https://doi.org/10.1016/S0012-821X(03)00721-0.

Frank, N., Ricard, E., Lutringer-Paquet, A., van der Land, C., Colin, C., Blamart, D., Foubert, A., Van Rooij, D., Henriet, J.-P., de Haas, H., van Weering, T., 2009. The Holocene occurrence of cold water corals in the NE Atlantic: implications for coral carbonate mound evolution. Mar. Geol. 266, 129–142. https://doi.org/10.1016/j.margeo.2009.08.007.

Freiwald, A., 2002. Reef-forming cold-water corals. In: Wefer, G., Billett, D., Hebbeln, D., Jorgensen, B., Schluter, M., van Weering, T. (Eds.), Ocean Margin Systems. Springer Berlin Heidelberg, Berlin, Heidelberg, pp. 365–385. https://doi.org/10.1007/978-3-662-05127-6_23.

García-Ibáñez, M.I., Pardo, P.C., Carracedo, L.I., Mercier, H., Lherminier, P., Ríos, A.F., Pérez, F.F., 2015. Structure, transports and transformations of the water masses in the Atlantic Subpolar Gyre. Prog. Oceanogr. 135, 18–36. https://doi.org/10.1016/j.pocean.2015.03.009.

Guinotte, J.M., Orr, J., Cairns, S., Freiwald, A., Morgan, L., George, R., 2006. Will human-induced changes in seawater chemistry alter the distribution of deep-sea scleractinian corals? Front. Ecol. Environ. 4, 141–146 https://doi.org/https://doi.org/10.1890/1540-9295(2006)004[0141:WHCISC]2.0.

Hanz, U., Wienberg, C., Hebbeln, D., Duineveld, G., Lavaleye, M., Juva, K., Dullo, W.-C., Freiwald, A., Tamborrino, L., Reichart, G.-J., Flögel, S., Mienis, F., 2019. Environmental factors influencing benthic communities in the oxygen minimum zones on the Angolan and Namibian margins. Biogeosciences 16, 4337–4356. https://doi.org/10.5194/bg-16-4337-2019.

Heaton, T.J., Köhler, P., Butzin, M., Bard, E., Reimer, R.W., Austin, W.E.N., Bronk Ramsey, C., Grootes, P.M., Hughen, K.A., Kromer, B., Reimer, P.J., Adkins, J., Burke, A., Cook, M.S., Olsen, J., Skinner, L.C., 2020. Marine20 - the marine radiocarbon age calibration curve (0-55,000 cal BP). Radiocarbon 62, 779–820. https://doi.org/10.1017/RDC.2020.68.

Hebbeln, D., Portilho-Ramos, R. da C., Wienberg, C., Titschack, J., 2019. The fate of cold-water corals in a changing world: a geological perspective. Front. Mar. Sci. 6, 1–8. https://doi.org/10.3389/fmars.2019.00119.

Hebbeln, D., Wienberg, C., Dullo, W.-C., Freiwald, A., Mienis, F., Orejas, C., Titschack, J., 2020. Cold-water coral reefs thriving under hypoxia. Coral Reefs 39, 853–859. https://doi.org/10.1007/s00338-020-01934-6.

Henderson, G.M., 2002. Seawater ($^{234}U/^{238}U$) during the last 800 thousand years. Earth Planet Sci. Lett. 199, 97–110. https://doi.org/10.1016/S0012-821X(02)00556-3.

Henry, L.-A., Frank, N., Hebbeln, D., Wienberg, C., Robinson, L., de Flierdt, T. van, Dahl, M., Douarin, M., Morrison, C.L., López Correa, M., Rogers, A.D., Ruckelshausen, M., Roberts, J.M., 2014. Global ocean conveyor lowers extinction risk in the deep sea. Deep-Sea Res. Part I Oceanogr. Res. Pap. 88, 8–16. https://doi.org/10.1016/j.dsr.2014.03.004.

Hernández-Guerra, A., Fraile-Nuez, E., López-Laatzen, F., Martínez, A., Parrilla, G., Vélez-Belchí, P., 2005. Canary current and North equatorial current from an inverse box model. J. Geophys. Res. 110, C12019 https://doi.org/10.1029/2005JC003032.

Hughes, A.L.C., Gyllencreutz, R., Lohne, Ø.S., Mangerud, J., Svendsen, J.I., 2016. The last Eurasian ice sheets - a chronological database and time-slice reconstruction, DATED-1. Boreas 45, 1–45. https://doi.org/10.1111/bor.12142.

Karakaş, G., Nowald, N., Blaas, M., Marchesiello, P., Frickenhaus, S., Schlitzer, R., 2006. High-resolution modeling of sediment erosion and particle transport across the northwest African shelf. J. Geophys. Res. Ocean. 111, 1–13. https://doi.org/10.1029/2005JC003296.

Lindberg, B., Mienert, J., 2006. Sedimentological and geochemical environment of the Fugløy Reef off northern Norway. Cold Water Coral Ecosyst. 633–650. https://doi.org/10.1007/3-540-27673-4_31.

Löfverström, M., Caballero, R., Nilsson, J., Kleman, J., 2014. Evolution of the large-scale atmospheric circulation in response to changing ice sheets over the last glacial cycle. Clim. Past 10, 1453–1471. https://doi.org/10.5194/cp-10-1453-2014.

López Correa, M., Montagna, P., Joseph, N., Rüggeberg, A., Fietzke, J., Flögel, S., Dorschel, B., Goldstein, S.L., Wheeler, A., Freiwald, A., 2012. Preboreal onset of cold-water coral growth beyond the Arctic Circle revealed by coupled radiocarbon and U-series dating and neodymium isotopes. Quat. Sci. Rev. 34, 24–43. https://doi.org/10.1016/j.quascirev.2011.12.005.

Mangini, A., Lomitschka, M., Eichstädter, R., Frank, N., Vogler, S., Bonani, G., Hajdas, I., Patzold, J., 1998. Coral provides way to age deep water. Nature 392, 347–348. https://doi.org/10.1038/32804.

Margolin, A.R., Robinson, L.F., Burke, A., Waller, R.G., Scanlon, K.M., Roberts, M.L., Auro, M.E., van de Flierdt, T., 2014. Temporal and spatial distributions of cold-water

corals in the Drake Passage: insights from the last 35,000 years. Deep. Res. Part II Top. Stud. Oceanogr. 99, 237–248. https://doi.org/10.1016/j.dsr2.2013.06.008.
Mark Moore, C., Mills, M.M., Achterberg, E.P., Geider, R.J., LaRoche, J., Lucas, M.I., McDonagh, E.L., Pan, X., Poulton, A.J., Rijkenberg, M.J.A., Suggett, D.J., Ussher, S. J., Woodward, E.M.S., 2009. Large-scale distribution of Atlantic nitrogen fixation controlled by iron availability. Nat. Geosci. 2, 867–871. https://doi.org/10.1038/ngeo667.
Matul, A., Barash, M.S., Khusid, T.A., Behera, P., Tiwari, M., 2018. Paleoenvironment variability during termination I at the Reykjanes Ridge, North Atlantic. Geosci. 8, 1–14. https://doi.org/10.3390/geosciences8100375.
McGee, D., DeMenocal, P.B., Winckler, G., Stuut, J.B.W., Bradtmiller, L.I., 2013. The magnitude, timing and abruptness of changes in North African dust deposition over the last 20,000yr. Earth Planet Sci. Lett. 371–372, 163–176. https://doi.org/10.1016/j.epsl.2013.03.054.
McKay, C.L., Filipsson, H.L., Romero, O.E., Stuut, J.B.W., Donner, B., 2014. Pelagic-benthic coupling within an upwelling system of the subtropical northeast Atlantic over the last 35kaBP. Quat. Sci. Rev. 106, 299–315. https://doi.org/10.1016/j.quascirev.2014.04.027.
Middleton, J.L., Mukhopadhyay, S., Langmuir, C.H., McManus, J.F., Huybers, P.J., 2018. Millennial-scale variations in dustiness recorded in Mid-Atlantic sediments from 0 to 70 ka. Earth Planet Sci. Lett. 482, 12–22. https://doi.org/10.1016/j.epsl.2017.10.034.
Mienis, F., van der Land, C., de Stigter, H.C., van de Vorstenbosch, M., de Haas, H., Richter, T., van Weering, T.C.E., 2009. Sediment accumulation on a cold-water carbonate mound at the Southwest Rockall Trough margin. Mar. Geol. 265, 40–50. https://doi.org/10.1016/j.margeo.2009.06.014.
Miller, K.J., Rowden, A.A., Williams, A., Häussermann, V., 2011. Out of their depth? Isolated deep populations of the cosmopolitan coral *desmophyllum dianthus* may be highly vulnerable to environmental change. PLoS One 6. https://doi.org/10.1371/journal.pone.0019004.
Mohn, C., Rengstorf, A., White, M., Duineveld, G., Mienis, F., Soetaert, K., Grehan, A., 2014. Linking benthic hydrodynamics and cold-water coral occurrences: a high-resolution model study at three cold-water coral provinces in the NE Atlantic. Prog. Oceanogr. 122, 92–104. https://doi.org/10.1016/j.pocean.2013.12.003.
Morato, T., González-Irusta, J., Dominguez-Carrió, C., Wei, C., Davies, A., Sweetman, A. K., Taranto, G.H., Beazley, L., García-Alegre, A., Grehan, A., Laffargue, P., Murillo, F. J., Sacau, M., Vaz, S., Kenchington, E., Arnaud-Haond, S., Callery, O., Chimienti, G., Cordes, E., Egilsdottir, H., Freiwald, A., Gasbarro, R., Gutiérrez-Zárate, C., Gianni, M., Gilkinson, K., Wareham Hayes, V.E., Hebbeln, D., Hedges, K., Henry, L., Johnson, D., Koen-Alonso, M., Lirette, C., Mastrototaro, F., Menot, L., Molodtsova, T., Durán Muñoz, P., Orejas, C., Pennino, M.G., Puerta, P., Ragnarsson, S.Á., Ramiro-Sánchez, B., Rice, J., Rivera, J., Roberts, J.M., Ross, S.W., Rueda, J.L., Sampaio, Í., Snelgrove, P., Stirling, D., Treble, M.A., Urra, J., Vad, J., Oevelen, D., Watling, L., Walkusz, W., Wienberg, C., Woillez, M., Levin, L.A., Carreiro-Silva, M., 2020. Climate-induced changes in the suitable habitat of cold-water corals and commercially important deep-sea fishes in the North Atlantic. Global Change Biol. 26, 2181–2202. https://doi.org/10.1111/gcb.14996.
Moros, M., Jansen, E., Oppo, D.W., Giraudeau, J., Kuijpers, A., 2012. Reconstruction of the late-holocene changes in the sub-arctic front position at the Reykjanes Ridge, North Atlantic. Holocene 22, 877–886. https://doi.org/10.1177/0959683611434224.
Mortensen, P.B., Buhl-Mortensen, L., Gebruk, A.V., Krylova, E.M., 2008. Occurrence of deep-water corals on the Mid-Atlantic Ridge based on MAR-ECO data. Deep. Res. Part II Top. Stud. Oceanogr. 55, 142–152. https://doi.org/10.1016/j.dsr2.2007.09.018.
Murton, B.J., 2016. MarineE-Tech Project: to Map the Cobalt-Rich Ferromanganese Crusts of Tropic Seamount , NE Atlantic Ocean Ocean.
Olsen, A., Lange, N., Key, R.M., Tanhua, T., Bittig, H.C., Kozyr, A., Álvarez, M., Azetsu-Scott, K., Becker, S., Brown, P.J., Carter, B.R., Cotrim Da Cunha, L., Feely, R.A., Van Heuven, S., Hoppema, M., Ishii, M., Jeansson, E., Jutterström, S., Landa, C.S., Lauvset, S.K., Michaelis, P., Murata, A., Pérez, F.F., Pfeil, B., Schirnick, C., Steinfeldt, R., Suzuki, T., Tilbrook, B., Velo, A., Wanninkhof, R., Woosley, R.J., 2020. An updated version of the global interior ocean biogeochemical data product. Earth Syst. Sci. Data 12, 3653–3678. https://doi.org/10.5194/essd-12-3653-2020. GLODAPv2.2020.
Orejas, C., Wienberg, C., Titschack, J., Tamborrino, L., Freiwald, A., Hebbeln, D., 2021. *Madrepora oculata* forms large frameworks in hypoxic waters off Angola (SE Atlantic). Sci. Rep. 11, 15170 https://doi.org/10.1038/s41598-021-94579-6.
Pastor, M.V., Vélez-Belchí, P., Hernández-Guerra, A., 2015. Water masses in the canary current large marine ecosystem. In: Valdés, L., Déniz-Golzáles, I. (Eds.), Oceanographic and Biological Features in the Canary Current Large Marine Ecosystem. IOC-UNESCO, Paris, pp. 73–79.
Pflaumann, U., Sarnthein, M., Chapman, M., d'Abreu, L., Funnell, B., Huels, M., Kiefer, T., Maslin, M., Schulz, H., Swallow, J., van Kreveld, S., Vautravers, M., Vogelsang, E., Weinelt, M., 2003. Glacial North Atlantic: sea-surface conditions reconstructed by GLAMAP 2000. Paleoceanography 18. https://doi.org/10.1029/2002pa000774.
Portilho-Ramos, R. da C., Titschack, J., Wienberg, C., Siccha Rojas, M.G., Yokoyama, Y., Hebbeln, D., 2022. Major environmental drivers determining life and death of cold-water corals through time. PLoS Biol. 20 https://doi.org/10.1371/journal.pbio.3001628.
Raddatz, J., Liebetrau, V., Trotter, J., Rüggeberg, A., Flögel, S., Dullo, W.-C., Eisenhauer, A., Voigt, S., McCulloch, M., 2016. Environmental constraints on Holocene cold-water coral reef growth off Norway: insights from a multiproxy approach. Paleoceanography 31, 1350–1367. https://doi.org/10.1002/2016PA002974.
Ramiro-Sánchez, B., González-Irusta, J.M., Henry, L.-A., Cleland, J., Yeo, I., Xavier, J.R., Carreiro-Silva, M., Sampaio, Í., Spearman, J., Victorero, L., Messing, C.G., Kazanidis, G., Roberts, J.M., Murton, B., 2019. Characterization and mapping of a deep-sea sponge ground on the tropic seamount (northeast tropical atlantic): implications for spatial management in the high seas. Front. Mar. Sci. 6, 1–19. https://doi.org/10.3389/fmars.2019.00278.
Rhein, M., Fischer, J., Smethie, W.M., Smythe-Wright, D., Weiss, R.F., Mertens, C., Min, D.-H., Fleischmann, U., Putzka, A., 2002. Labrador Sea water: pathways, CFC inventory, and formation rates. J. Phys. Oceanogr. 32, 648–665. https://doi.org/10.1175/1520-0485(2002)032<0648:LSWPCI>2.0.CO.
Roberts, J.M., Wheeler, A.J., Freiwald, A., 2006. Reefs of the deep: the biology and geology of cold-water coral ecosystems. Science 312, 543–547. https://doi.org/10.1126/science.1119861.
Robinson, L.F., 2014. RRS james cook cruise JC094, october 13 - novemeber 30 2013, tenerife - trinidad. TROPICS, tracing oceanic processes using corals and sediments. In: Reconstructing abrupt Changes in Chemistry and Circulation of the Equatorial Atlantic Ocean: Implications for global Climate and deep-water Habitats.
Robinson, L.F., Adkins, J.F., Fernandez, D.P., Burnett, D.S., Wang, S.L., Gagnon, A.C., Krakauer, N., 2006. Primary U distribution in scleractinian corals and its implications for U series dating. G-cubed 7. https://doi.org/10.1029/2005GC001138.
Robinson, L.F., Adkins, J.F., Keigwin, L.D., Southon, J., Fernandez, D.P., Wang, S.L., Scheirer, D.S., 2005. Radiocarbon variability in the western North Atlantic during the last deglaciation. Science 310, 1469–1473. https://doi.org/10.1126/science.1114832.
Rogerson, M., Rohling, E.J., Weaver, P.P.E., Murray, J.W., 2005. Glacial to interglacial changes in the settling depth of the Mediterranean Outflow plume. Paleoceanography 20, 1–12. https://doi.org/10.1029/2004PA001106.
Romero, O.E., Kim, J.-H., Donner, B., 2008. Submillennial-to-millennial variability of diatom production off Mauritania, NW Africa, during the last glacial cycle. Paleoceanography 23. https://doi.org/10.1029/2008PA001601.
Rowland, G.H., Robinson, L.F., Hendry, K.R., Ng, H.C., McGee, D., McManus, J.F., 2021. The spatial distribution of aeolian dust and terrigenous fluxes in the tropical Atlantic Ocean since the last glacial maximum. Paleoceanogr. Paleoclimatol. 36, 1–17. https://doi.org/10.1029/2020PA004148.
Santos, G.C., Kerr, R., Azevedo, J.L.L., Mendes, C.R.B., da Cunha, L.C., 2016. Influence of antarctic intermediate water on the deoxygenation of the Atlantic Ocean. Dynam. Atmos. Oceans 76, 72–82. https://doi.org/10.1016/j.dynatmoce.2016.09.002.
Schröder-Ritzrau, A., Freiwald, André, Mangini, A., 2005. U/Th-dating of deep-water corals from the eastern North Atlantic and the western Mediterranean Sea. In: Freiwald, A., Roberts, J.M. (Eds.), Cold-Water Corals and Ecosystems. Springer-Verlag, Berlin/Heidelberg, pp. 157–172. https://doi.org/10.1007/3-540-27673-4_8.
Schröder-Ritzrau, A., Mangini, A., Lomitschka, M., 2003. Deep-sea corals evidence periodic reduced ventilation in the North Atlantic during the LGM/Holocene transition. Earth Planet Sci. Lett. 216, 399–410. https://doi.org/10.1016/S0012-821X(03)00511-9.
Sigman, D.M., Hain, M.P., 2012. The biological productivity of the ocean. Nat. Educ. Knowl. 3, 10–21.
Spooner, P.T., Chen, T., Robinson, L.F., Coath, C.D., 2016. Rapid uranium-series age screening of carbonates by laser ablation mass spectrometry. Quat. Geochronol. 31, 28–39. https://doi.org/10.1016/j.quageo.2015.10.004.
Spratt, R.M., Lisiecki, L.E., 2016. A Late Pleistocene sea level stack. Clim. Past 12, 1079–1092. https://doi.org/10.5194/cp-12-1079-2016.
Stewart, J.A., Li, T., Spooner, P.T., Burke, A., Chen, T., Roberts, J., Rae, J.W.B., Peck, V., Kender, S., Liu, Q., Robinson, L.F., 2021. Productivity and dissolved oxygen controls on the Southern Ocean deep-sea benthos during the antarctic cold reversal. Paleoceanogr. Paleoclimatol. 36 https://doi.org/10.1029/2021PA004288.
Thiagarajan, N., Gerlach, D., Roberts, M.L., Burke, A., McNichol, A., Jenkins, W.J., Subhas, A.V., Thresher, R.E., Adkins, J.F., 2013. Movement of deep-sea coral populations on climatic timescales. Paleoceanography 28, 227–236. https://doi.org/10.1002/palo.20023.
Thornalley, D.J.R., Elderfield, H., McCave, I.N., 2011. Reconstructing North Atlantic deglacial surface hydrography and its link to the Atlantic overturning circulation. Global Planet. Change 79, 163–175. https://doi.org/10.1016/j.gloplacha.2010.06.003.
Titschack, J., Baum, D., De Pol-Holz, R., López Correa, M., Forster, N., Flögel, S., Hebbeln, D., Freiwald, A., 2015. Aggradation and carbonate accumulation of Holocene Norwegian cold-water coral reefs. Sedimentology 62, 1873–1898. https://doi.org/10.1111/sed.12206.
Toucanne, S., Soulet, G., Vázquez Riveiros, N., Boswell, S.M., Dennielou, B., Waelbroeck, C., Bayon, G., Mojtahid, M., Bosq, M., Sabine, M., Zaragosi, S., Bourillet, J., Mercier, H., 2021. the North atlantic glacial eastern boundary current as a key driver for ice-sheet—AMOC interactions and climate instability. Paleoceanogr. Paleoclimatol. 36, 1–23. https://doi.org/10.1029/2020PA004068.
van der Land, C., Eisele, M., Mienis, F., de Haas, H., Hebbeln, D., Reijmer, J.J.G., van Weering, T.C.E., 2014. Carbonate mound development in contrasting settings on the Irish margin. Deep Sea Res. Part II Top. Stud. Oceanogr. 99, 297–306. https://doi.org/10.1016/j.dsr2.2013.10.004.
van der Land, C., Mienis, F., de Haas, H., Frank, N., Swennen, R., van Weering, T.C.E., 2010. Diagenetic processes in carbonate mound sediments at the south-west Rockall Trough margin. Sedimentology 57, 912–931. https://doi.org/10.1111/j.1365-3091.2009.01125.x.
Vernet, M., Ellingsen, I.H., Seuthe, L., Slagstad, D., Cape, M.R., Matrai, P.A., 2019. Influence of phytoplankton advection on the productivity along the atlantic water inflow to the Arctic Ocean. Front. Mar. Sci. 6, 1–18. https://doi.org/10.3389/fmars.2019.00583.

Victorero, L., Blamart, D., Pons-Branchu, E., Mavrogordato, M.N., Huvenne, V.A.I., 2016. Reconstruction of the formation history of the Darwin Mounds, N Rockall Trough: how the dynamics of a sandy contourite affected cold-water coral growth. Mar. Geol. 378, 186–195. https://doi.org/10.1016/j.margeo.2015.12.001.

Victorero, L., Robert, K., Robinson, L.F., Taylor, M.L., Huvenne, V.A.I., 2018. Species replacement dominates megabenthos beta diversity in a remote seamount setting. Sci. Rep. 8, 1–11. https://doi.org/10.1038/s41598-018-22296-8.

Wagner, T., 2000. Control of organic carbon accumulation in the late Quaternary equatorial Atlantic (Ocean Drilling Program sites 664 and 663): productivity versus terrigenous supply. Paleoceanography 15, 181–199. https://doi.org/10.1029/1999PA000406.

Wienberg, C., Frank, N., Mertens, K.N., Stuut, J.-B., Marchant, M., Fietzke, J., Mienis, F., Hebbeln, D., 2010. Glacial cold-water coral growth in the Gulf of Cádiz: implications of increased palaeo-productivity. Earth Planet Sci. Lett. 298, 405–416. https://doi.org/10.1016/j.epsl.2010.08.017.

Wienberg, C., Hebbeln, D., Fink, H.G., Mienis, F., Dorschel, B., Vertino, A., Correa, M.L., Freiwald, A., 2009. Scleractinian cold-water corals in the Gulf of Cádiz—first clues about their spatial and temporal distribution. Deep-Sea Res. Part I Oceanogr. Res. Pap. 56, 1873–1893. https://doi.org/10.1016/j.dsr.2009.05.016.

Wienberg, C., Titschack, J., Frank, N., De Pol-Holz, R., Fietzke, J., Eisele, M., Kremer, A., Hebbeln, D., 2020. Deglacial upslope shift of NE Atlantic intermediate waters controlled slope erosion and cold-water coral mound formation (Porcupine Seabight, Irish margin). Quat. Sci. Rev. 237, 106310 https://doi.org/10.1016/j.quascirev.2020.106310.

Wienberg, C., Titschack, J., Freiwald, A., Frank, N., Lundälv, T., Taviani, M., Beuck, L., Schröder-Ritzrau, A., Krengel, T., Hebbeln, D., 2018. The giant Mauritanian cold-water coral mound province: oxygen control on coral mound formation. Quat. Sci. Rev. 185, 135–152. https://doi.org/10.1016/j.quascirev.2018.02.012.

Xiao, X., Zhao, M., Knudsen, K.L., Sha, L., Eiríksson, J., Gudmundsdóttir, E., Jiang, H., Guo, Z., 2017. Deglacial and Holocene sea–ice variability north of Iceland and response to ocean circulation changes. Earth Planet Sci. Lett. 472, 14–24. https://doi.org/10.1016/j.epsl.2017.05.006.

Zarriess, M., Mackensen, A., 2010. The tropical rainbelt and productivity changes off northwest Africa: a 31,000-year high-resolution record. Mar. Micropaleontol. 76, 76–91. https://doi.org/10.1016/j.marmicro.2010.06.001.